TOD: GPU-accelerated Outlier Detection via Tensor Operations

Yue Zhao
Carnegie Mellon University
Pittsburgh, PA
zhaoy@cmu.edu

George H. Chen
Carnegie Mellon University
Pittsburgh, PA
georgechen@cmu.edu

Zhihao Jia
Carnegie Mellon University
Pittsburgh, PA
zhihao@cmu.edu

ABSTRACT

Outlier detection (OD) is a key machine learning task for finding rare and deviant data samples, with many time-critical applications such as fraud detection and intrusion detection. In this work, we propose TOD, the first tensor-based system for efficient and scalable outlier detection on distributed multi-GPU machines. A key idea behind TOD is decomposing complex OD applications into a small collection of basic tensor algebra operators. This decomposition enables TOD to accelerate OD computations by leveraging recent advances in deep learning infrastructure in both hardware and software. Moreover, to deploy memory-intensive OD applications on modern GPUs with limited on-device memory, we introduce two key techniques. First, *provable quantization* speeds up OD computations and reduces its memory footprint by automatically performing specific floating-point operations in lower precision while provably guaranteeing no accuracy loss. Second, to exploit the aggregated compute resources and memory capacity of multiple GPUs, we introduce *automatic batching*, which decomposes OD computations into small batches for both sequential execution on a single GPU and parallel execution across multiple GPUs.

TOD supports a diverse set of OD algorithms. Evaluation on 11 real-world and 3 synthetic OD datasets shows that TOD is on average 10.9× faster than the leading CPU-based OD system PyOD (with a maximum speedup of 38.9×), and can handle much larger datasets than existing GPU-based OD systems. In addition, TOD allows easy integration of new OD operators, enabling fast prototyping of emerging and yet-to-discovered OD algorithms.

PVLDB Reference Format:
Yue Zhao, George H. Chen, and Zhihao Jia. TOD: GPU-accelerated Outlier Detection via Tensor Operations. PVLDB, 16(3): 546 - 560, 2022.
doi:10.14778/3570690.3570703

PVLDB Artifact Availability:
The source code, data, and/or other artifacts have been made available at https://github.com/yzhao062/pytod.

1 INTRODUCTION

Outlier detection (OD) is a crucial machine learning task for identifying data points deviating from a general distribution [4, 56, 99]. OD has numerous real-world applications, including anti-money laundering [48], rare disease detection [74], rumor detection [88], and network intrusion detection [45]. OD algorithms have been serving a critical role in large cloud services for monitoring server abnormality at Microsoft [80] and Amazon [11], as well as for fraud detection at eBay [2] and Alibaba [54].

Scalability challenges of OD. Numerous OD algorithms have been proposed recently to detect outliers for different types of data (e.g., tabular data [4, 41, 53, 104], time series [16, 18, 23, 44], and graphs [5, 17]). Although there is no shortage of detection algorithms, OD applications face challenges in *scaling to large datasets*, both in terms of execution time and memory consumption, which prevents OD algorithms from being deployed in data-intensive and/or time-critical tasks such as real-time credit card fraud detection. To address these challenges, recent work focuses on both developing distributed OD algorithms on CPUs [8, 13, 61, 71, 73, 90, 97, 101, 103] and accelerating certain OD algorithms on GPUs [9, 46]. However, existing GPU-based OD solutions only target specific (families of) OD algorithms and cannot support *generic* OD computations. For instance, Angiulli et al. [9] showcases an example of using GPUs for distance-based algorithms, while how to handle linear and probabilistic OD algorithms remains unclear in the proposed solution.

Advances in systems for deep neural networks. On the other hand, deep neural networks (DNNs) have revolutionized computer vision, natural language processing, and various other fields [32] over the last decade. This success is largely due to the recent development of DNN systems (e.g., TensorFlow [1] and PyTorch [76]). These systems enable fast tensor algebra computations (e.g., matrix multiplication, convolution, etc.) on modern hardware accelerators (e.g., GPUs and TPUs) and use efficient parallelization strategies (e.g., data, model, and pipeline parallelism [39, 68, 92]) to aggregate the compute resources across multiple accelerators, enabling efficient and scalable DNN computations.

This paper explores a new approach to building GPU-accelerated OD systems. Instead of following the methodology used in existing GPU-based OD frameworks (i.e., providing efficient GPU implementations tailored to specific OD applications), we ask: *can we leverage the compilation and optimization techniques in DNN systems to minimize the time and memory consumption of a wide range of common OD computations?*

1.1 Our Approach

In this paper, we present TOD, a tensor-based outlier detection system that abstracts OD applications into tensor algebra operations for efficient GPU acceleration. TOD leverages both the software and hardware optimizations in modern DNN frameworks to enable efficient and scalable OD computations on distributed multi-GPU clusters. To the best of our knowledge, TOD is the *first* GPU-based system for *generic* OD applications. Fig. 1 shows an overview of TOD. Building a tensor-based OD system requires addressing three major obstacles.

Proceedings of the VLDB Endowment, Vol. 16, No. 3 ISSN 2150-8097.
doi:10.14778/3570690.3570703

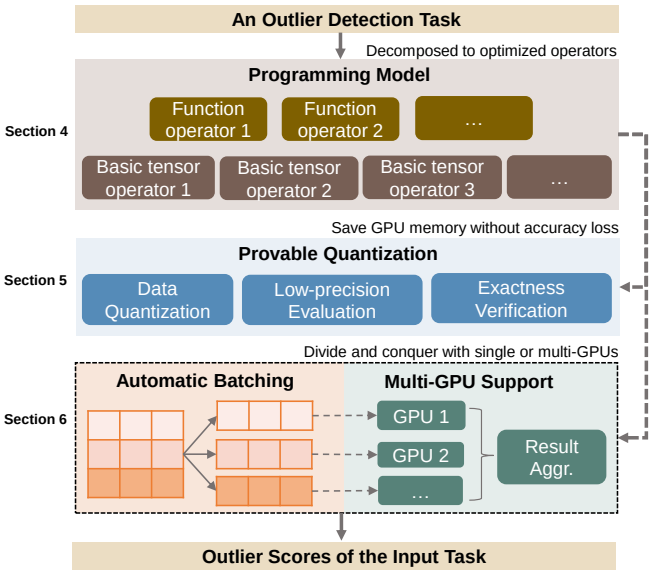

Figure 1: TOD's overview. TOD decomposes an OD task into fine-grained tensor operators and optimizes OD computations across multiple GPUs using provable quantization and automatic batching.

Representing OD computations using tensor operations. Unlike DNN models, which are represented as a pipeline of tensor algebra operators (e.g., matrix multiplication), many OD applications involve a diverse collection of operators that have traditionally not been implemented in terms of tensor operations, such as proximity-based algorithms, statistical approaches, and linear methods (see an overview of OD applications in §2.1). Implementing OD applications one at a time and accounting for software and hardware optimizations is labor-intensive. To address this obstacle, TOD introduces a new programming model for OD that decomposes a broad set of OD applications into a small collection of *basic tensor operators* and *functional operators*, which significantly reduces the implementation and optimization effort and opens the possibility of easily supporting new OD algorithms.

Quantizing OD computations. *Quantization* is commonly used in existing DNN frameworks to reduce the run time and memory consumption of DNN computations by computing intermediate results in a DNN model using a lower-precision floating-point representation. Quantization in general does not preserve the end-to-end equivalence of a DNN model and therefore may introduce potential accuracy losses. To apply quantization, the current practice is fine-tuning a quantized DNN model on the training dataset in a *supervised* fashion and assessing the accuracy loss; however, this approach is not directly applicable to OD, since most OD algorithms are *unsupervised* and thus lack a direct way for measuring accuracy. To address this challenge, TOD introduces a novel quantization technique called *provable quantization*, which leverages the numerical insensitivity of OD algorithms (e.g., k-nearest-neighbors may return identical results for some samples when computing with different floating-point precisions) and *automatically* performs specific OD operators in lower precision. In contrast to prior quantization techniques that use lower precision calculations at the expense of accuracy, provable quantization guarantees *no* accuracy loss.

Enabling scalable OD computations. Existing DNN frameworks cannot directly support large-scale OD applications, since modern DNN systems are designed to iteratively process a small *batch* of training samples even though the entire training dataset can be large. For example, to train ResNet-50 [35] on the ImageNet dataset [25], existing DNN systems only handle small mini-batches (e.g., 256 samples) in each training iteration, while the dataset contains more than 14 million samples. However, many OD applications involve operating on *all* samples, such as computing distances between all sample pairs. Executing such an application on a single GPU would typically run out of memory because GPUs nowadays have limited memory capacities (e.g., compared to those of CPU DRAM). To overcome the difficulty of executing OD applications in iterations and the resource limits of a single GPU, TOD uses an *automatic batching* mechanism to execute memory-intensive OD operators in small batches, which are distributed across *multiple* GPUs in parallel in a pipeline fashion. The automatic batching and multi-GPU support allow TOD to scale to datasets as large as those commonly encountered in deep learning tasks.

We compare TOD against existing CPU- and GPU-based OD systems on both real-world and synthetic datasets. TOD is on average 10.9× faster than PyOD, a state-of-the-art comprehensive CPU-based OD system [105], and can process a million samples within an hour while PyOD cannot. Compared to existing GPU-based OD systems, TOD can handle much larger datasets, while the GPU baselines run out of GPU memory. Our evaluation further shows that provable quantization, automatic batching, and multi-GPU support are all critical for efficient and scalable OD computations.

In summary, this paper makes the following contributions:

- We propose TOD, the first tensor-based system for generic outlier detection, enabling efficient and scalable OD computations on distributed multi-GPU machines.
- TOD uses a new programming model that abstracts complex OD applications into a small collection of basic tensor operators for efficient GPU acceleration.
- We introduce provable quantization that accelerates unsupervised OD computations by performing specific floating-point operators in lower precision while provably guaranteeing no accuracy loss.

Extensibility and integration. TOD is open-sourced[1] (see Appx. §D for an API demonstration), which enables easy development of new OD algorithms by leveraging highly optimized tensor operators or including new operators (see examples in §7.1). This extensibility yields a large number of yet-to-be-discovered OD methods. Thus, we believe that TOD also provides a platform that enables rapid research and development of new OD methods.

2 BACKGROUND AND RELATED WORK

In this section, §2.1 summarizes existing OD algorithms for tabular data, §2.2 introduces existing DNN infrastructure, which is leveraged by TOD to accelerate OD computations, and §2.3 describes modern OD systems. In §2.4, we review additional systems, algorithms, and applications for other data formats in addition to

[1]Open-sourced library and online appendix: https://github.com/yzhao062/pytod

Table 1: Key OD algorithms for tabular data and their time and space complexity with a *brute-force* implementation (additional optimization is possible but not considered here), where n is the number of samples, and d is the number of dimensions. Note that ensemble-based methods' complexities depend on the underlying base estimators. Algorithms that can be accelerated in TOD are marked with ✓.

Category	Algorithm	Time Compl.	Space Compl.	Optimized in TOD
Proximity	kNNOD	$O(n^2)$	$O(n^2)$	✓
Proximity	COF	$O(n^3)$	$O(n^2)$	✓
Proximity	LOF	$O(n^2)$	$O(n^2)$	✓
Proximity	LOCI	$O(n^2)$	$O(n^2)$	✓
Statistical	KDE	$O(n^3)$	$O(n^2)$	✗
Statistical	HBOS	$O(nd)$	$O(nd)$	✓
Statistical	COPOD	$O(nd)$	$O(nd)$	✓
Statistical	ECOD	$O(nd)$	$O(nd)$	✓
Ensemble	LODA	N/A	N/A	✓
Ensemble	FB	N/A	N/A	✓
Ensemble	iForest	N/A	N/A	✗
Ensemble	LSCP	N/A	N/A	✓
Linear	PCA	$O(nd)$	$O(n)$	✓
Linear	OCSVM	$O(n^3)$	$O(n^2)$	✗

tabular data (e.g., time series and graphs). Note that TOD primarily focuses on OD in tabular data due to its popularity [4]; TOD can be extended to support OD in other data types with modifications.

2.1 Existing OD Algorithms and Scalability

Outlier detection (also called anomaly detection) is a key machine learning task that aims to find data points that deviate from a general distribution [4, 56, 99]. As shown in Table 1, non-deep-learning OD algorithms are grouped into four categories (see the book by Aggarwal [4] for more details on algorithms): (*i*) proximity-based algorithms that rely on measuring sample similarity including kNN [10], ABOD [43], COF [89], LOF [19], and LOCI [75]; (*ii*) statistical approaches including KDE [84], HBOS [31], COPOD [52], and ECOD [53]; (*iii*) ensemble-based methods that build a collection of detectors for aggregation like iForest [55], LODA [78], and LCSP [104]; and (*iv*) linear models such as PCA [85].

Many OD algorithms suffer from scalability issues [72, 103]. For example, Table 1 shows that various proximity-based OD algorithms have at least $O(n^2)$ time and space complexities—they all require estimating and storing pairwise distances among all n samples. The high time complexities of many OD algorithms limit their applicability in real-world applications that require either real-time responses (e.g., fraud detection [59]) or the concurrent processing of millions of samples [106]. As shown in the table, TOD supports nearly all the OD algorithms mentioned.

2.2 DNN Infrastructure and Acceleration

Deep neural networks have dramatically improved the accuracy of artificial intelligence systems across numerous fields [28, 32, 74]. Its success is fueled by recent advances in both DNN hardware and software [47]. Specifically, DNN systems depend on tensor operations that can often be parallelized and executed in small batches. These operations are well-suited for GPUs, especially as a single GPU nowadays often has many more cores than a single CPU; while GPU cores are not as general purpose as CPU cores, they suffice in executing the tensor operations of deep learning. Moreover, the maturity of DNN programming frameworks such as PyTorch [76] and TensorFlow [1] makes developing machine learning models easy with a wide range of GPUs. Multiple works attempt to leverage DNN systems for accelerating training data science and ML tasks, including Hummingbird [67], Tensors [42], and AC-DBSCAN [37].

Differently, TOD for the first time, extends the acceleration usage of DNN systems to OD algorithms. We build TOD using the DNN ecosystem, taking advantage of its established hardware acceleration and software accessibility. This design choice also opens the opportunity for unifying classical OD algorithms (see §2.1) and DNN-based OD algorithms on the same platform—this emerging direction has gained increasing attention in OD research [82].

2.3 Outlier Detection Systems

CPU-based systems . Over the years, comprehensive OD systems on CPUs that cover a diverse group of algorithms have been developed in different programming languages, including ELKI Data Mining [3] and RapidMiner [81] in Java, and PyOD [105] in Python. Among these, PyOD is the state-of-the-art (SOTA) with deep optimization including just-in-time compilation and parallelization. It is widely used in both academia and industry, with hundreds of citations [102] and millions of downloads per year [86]. Recently, the PyOD team proposed an acceleration system called SUOD to further speed up the training and prediction in PyOD with a large collection of heterogeneous OD models [103]. Specifically, SUOD uses algorithmic approximation and efficient parallelization to reduce the computational cost and therefore runtime. There are other distributed/parallel systems designed for specific (family of) OD algorithms with non-GPU nodes (e.g., CPUs): (*i*) Parallel Bay, Parallel LOF, DLOF for local OD algorithms [61, 71, 97], (*ii*) DOoR for distance-based OD [13], (*iii*) distributed OD for mixed-attributed data [73] (*iv*) PROUD for stream data [90] and (*v*) Sparx for Apache Spark [101]. These distributed non-GPU systems do not constitute as baselines as TOD is a comprehensive system covering different types OD algorithms, while the specialized systems only cover specific algorithms. Thus, we consider the SOTA comprehensive system, PyOD, as the primary baseline (see exp. results in §7.3).

GPU-based systems . There are efforts to use GPUs for fast OD calculations for LOF [6], distance-based methods [9], KDE [12], and data stream [46]. These approaches rely on exploring the characteristics of a specific OD algorithm for GPU acceleration. This limits their generalization to a wide collection of OD algorithms. Furthermore, none has direct multi-GPU support, leading to limited scalability. To the best of our knowledge, there is no existing comprehensive GPU-based OD system that covers a diverse group of algorithms. Thus, we use direct GPU implementations of OD algorithms and selected works above as GPU baselines when appropriate (see details in §7.2 and Table 3).

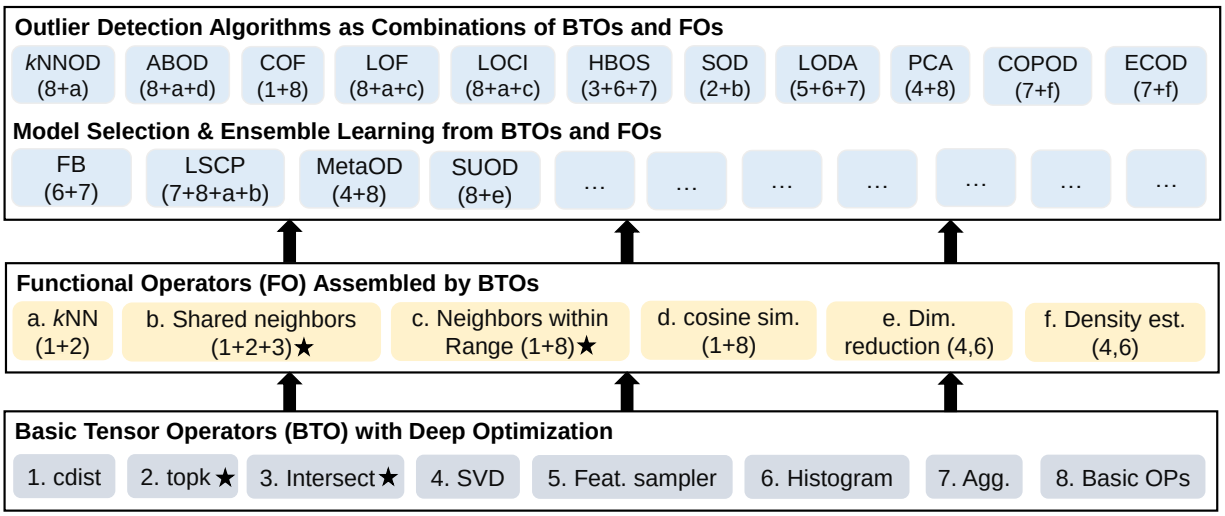

Figure 2: With algorithmic abstraction, more than 20 OD algorithms (denoted by) are abstracted into eight basic tensor operators (in) and six functional operators (in). This abstraction reduces the implementation and optimization effort, and opens the possibility of including new algorithms. All operators are executed on GPUs using automatic batching (see §6), and operators marked with ★ are further accelerated using provable quantization (see §5).

2.4 Systems for Other Data Types and Scenarios

Over the years, various algorithms and systems have been developed for OD with different types of data other than tabular, including time-series/sequence (TOP [23], NETS [98], GraphAn [17], CPOD [91], Series2graph [16], SAND [18], etc.), and graph (e.g., Elle [41], PyGOD [57, 58], etc.). Also, different input data are also assumed in streaming and feature-evolving fashions (e.g., xStream [62], etc.). Meanwhile, emphasis has also been given to building systems for explaining outliers (VSOutlier [22] and Exathlon [36], etc.) and outlier repairing (IMR [100], etc.), other than detecting them. In this paper, we focus on the detection task in the most prevalent setting (i.e., static tabular data) [4], while future works may extend to other data types and scenarios.

3 OVERVIEW

3.1 Definition and Problem Formulation

An OD system supports a collection of OD models $\mathcal{M} = \{M_1, ..., M_m\}$ such that given a user-specified OD model $M \in \mathcal{M}$ and an input dataset $\mathbf{X} \in \mathbb{R}^{n \times d}$ *without* ground truth labels (rows of $\mathbf{X}$ are data points, while columns are features), the system outputs outlier scores $\mathbf{O} := M(\mathbf{X}) \in \mathbb{R}^n$, which should be roughly deterministic and irrespective of the underlying system (higher values in $\mathbf{O}$ correspond to data points more likely to be identified as outliers; threshold on outlier scores can be used to determine which points are outliers). Given a hardware configuration C (e.g., CPUs and GPUs), the system's performance can be measured in *efficiency* (both runtime and memory consumption).

3.2 TOD's Overview

TOD is a comprehensive (i.e., covering a diverse group of methods) OD system as outlined in Fig. 1 and Table 1. For an outlier detection task, TOD decomposes it into a combination of predefined tensor operators via the proposed *programming model* for direct GPU acceleration (§4). Notably, TOD opportunistically performs *provable quantization* on tensor operators to enable faster computation and reduce memory requirements, while provably maintaining model accuracy (§5). To overcome the resource limitation of a single GPU, we further introduce *automatic batching* and *multi-GPU* support in TOD (§6).

4 PROGRAMMING MODEL

Motivation. As a comprehensive system, TOD aims to include a diverse collection of OD algorithms, including proximity-based methods, statistical methods, and more (see §2.1). However, not all algorithms can be directly converted into tensor operations for GPU acceleration. A key design goal of TOD is to support various OD algorithms by piecing together commonly recurring building blocks. In particular, rather than manually implementing many OD algorithms, which is a labor-intensive process, we instead define OD algorithms as compositions of basic OD building blocks, each of which only needs to be implemented once. Moreover, the building blocks can be optimized independently.

4.1 Algorithmic Abstraction

The key idea of our programming model is to decompose existing OD algorithms into a set of low-level *basic tensor operators* (BTOs), which can directly benefit from GPU acceleration. On top of these BTOs, we introduce higher-level OD operators called *functional operators* (FOs) with richer semantics. Consequently, OD algorithms can be constructed as combinations of BTOs and FOs.

Fig. 2 shows the hierarchy of TOD's programming abstraction in a bottom-up way, with increasing dependency: 8 BTOs are first constructed as the foundation of TOD (shown at the bottom in gray),

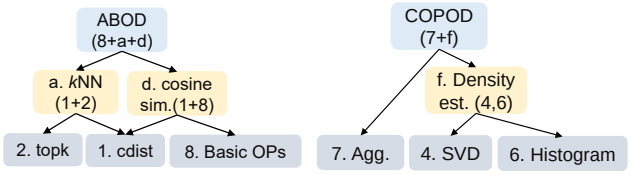

(a) Abstraction of ABOD **(b) Abstraction of COPOD**

Figure 3: Examples of building complex OD algorithms with FO and BTO conveniently.

while 6 FOs are then created on top of them (shown in the middle). Finally, OD algorithms and key functions on the top of the figure can be assembled using BTOs and FOs. In other words, TOD represents an OD algorithm using a tree-structured dependency graph, where the BTOs (as leaves of the tree) are fully independent for deep optimization, and all the algorithms depending on these BTOs can be collectively optimized. Clearly, this abstraction process reduces the repetitive implementation and optimization effort, and improves TOD's efficiency and generalizability. Additionally, it also facilities fast prototyping and experimentation with new algorithms.

4.2 Building End-to-end OD Algorithms

It is easy to build an end-to-end OD application by constructing its computation graph using FOs and BTOs. For instance, angle-based outlier detection (ABOD) is a classical OD algorithm [43], where each sample's outlier score is calculated as the average cosine similarity of its neighbors. Fig. 3(a) highlights an implementation of ABOD that uses an FO (i.e., *k*NN) to obtain a list of neighbors for each sample and then applies another FO (i.e., `cosine sim.`) for calculating cosine similarity. Note that each FO is a combination of BTOs. For example, *k*NN is implemented as calculating pairwise sample distance using `cdist` and then identifying the k "neighbor" with smallest distances using `topk`. Additionally, Fig. 3(b) shows the abstraction graph of copula-based outlier detection (COPOD) [52]. Other OD algorithms follow the same abstraction protocol and are represented as combinations of BTOs and FOs.

5 PROVABLE QUANTIZATION

Motivation. OD operators mainly depend on floating-point arithmetic, namely $\{+, -, \times, /\}$. For these operations, the main source of imprecision is rounding [50]. Rounding errors enlarge when storing numbers using fewer bits, e.g., 16-bit floating-points lead to more inaccuracy than 64-bit floating-points. Therefore, many machine learning algorithms use high-precision floating-points when possible to minimize the impact of rounding errors. However, using high-precision floating-points can increase computation time and memory consumption. This is especially critical for GPUs with limited memory.

To reduce memory usage and run time, *quantization* has been applied to many machine learning algorithms [14] and data-driven applications [7, 95, 96]. Simply put, it refers to executing an operator (function) with lower-precision floating representations. If we denote the original function by $r(x)$ and its quantization by $r_q(x)$, the rounding error $\mathrm{Err}(\cdot)$ of quantization is defined as the output difference between $r(x)$ and $r_q(x)$, namely $\mathrm{Err}(r_q(x)) = r(x) - r_q(x)$. Intuitively, quantization can save memory at the cost of accuracy. How to balance the tradeoff between the *memory cost* and *algorithm accuracy* is a key challenge for quantizing in machine learning [24]. In supervised ML, one may measure the inaccuracy caused by quantization using ground truth labels. However, this is infeasible under unsupervised OD settings, where no ground truth labels is available for evaluation as described in §3. Thus, existing quantization techniques for supervised ML do not suit the need of unsupervised OD.

In TOD, we design a correctness-preserving quantization technique for (unsupervised) OD applications, termed *provable quantization*. The key idea behind provable quantization is that depending on the operator used, it is possible to apply quantization to reduce memory consumption with *no* loss in accuracy. As a motivating example, consider the sign function $r(x)$ that returns "+" if $x > 0$ and returns "−" otherwise. Clearly, even if we quantize x to have a single bit (that precisely indicates the sign of x), we can achieve an exact answer for $r(x)$ that is the same as if instead x had more bits. Similarly, the ranking between two floating-point numbers often only depends on the most significant digits. Building on this simple intuition, we introduce *provable quantization* for a collection of OD operators, where the output and accuracy of the operators remain provably unchanged before and after quantization.

5.1 $(1+\epsilon)$-property for Rounding Errors

Provable quantization relies on a standard analysis technique for floating-point numbers called the "$(1+\epsilon)$-property" [50]. Let $\mathbb{F}$ denote the set of 64-bit floating-point numbers. For $x, y \in \mathbb{F}$, we define the floating-point operation "$\circledast$" as $x \circledast y \triangleq \mathrm{fl}(x * y)$, where $* \in \{+, -, \times, /\}$ and $\mathrm{fl}(\cdot)$ refers to the IEEE 754 standard for rounding a real number to a 64-bit floating-point number [40]. For example, $\oplus$ is floating-point addition and $\otimes$ is floating-point multiplication. The standard technique for calculating the rounding errors in floating-point operations is the $(1+\epsilon)$-property [50], which is formally defined as follows.

Theorem 1 (Theorem 3.2 of Lee et al. 50). *Let $x, y \in \mathbb{F}$, and $* \in \{+, -, \times, /\}$. Suppose that $|x * y| \leq \max \mathbb{F}$. Then when we compute $x * y$ in floating-point, there exist multiplicative and additive error terms $\delta \in \mathbb{R}$ and $\delta' \in \mathbb{R}$ respectively such that*

$$x \circledast y = (x * y)(1+\delta) + \delta', \quad \text{where } |\delta| \leq \epsilon, |\delta'| \leq \epsilon'. \tag{1}$$

In the above equation, ϵ and ϵ' are constants that do not depend on x or y. For instance, when working with 64-bit floating-point numbers, $\epsilon = 2^{-53}$ and $\epsilon' = 2^{-1075}$.

As discussed by Lee et al. [50, Section 5], this property can be further simplified when the exact result of the floating operation is not in the so-called "subnormal" range: the addictive error term δ' can be soundly removed, leading to a simplified $(1+\epsilon)$-property:

$$x \circledast y = (x * y)(1+\delta), \quad \text{where } |\delta| \leq \epsilon. \tag{2}$$

5.2 Provable Quantization in TOD

TOD applies provable quantization for an applicable operator $r(\cdot)$ with input x in three steps: (*i*) input quantization, (*ii*) low-precision

evaluation, and (*iii*) exactness verification and, if needed, recalculation. In a nutshell, the input is first quantized into a lower precision, and then the operator is evaluated in the lower precision, where $r(x)$ is evaluated as $r_q(x)$. To verify the exactness of the quantization, we calculate the rounding error $\mathrm{Err}(r_q(x))$ by the simplified $(1+\epsilon)$-property in eq. (2) and then check whether the result of $r(x)$ may change with the rounding error. If it passes the verification, then we output $\mathrm{Err}(r_q(x))$ as the final result; otherwise, we use the original precision of x to recalculate $r(x)$. Note that we apply this technique to the entire input data $\mathbf{X} \in \mathbb{R}^{n\times d}$, and only need to recalculate on the subset of $\mathbf{X}$ where the verification fails. A limitation of provable quantization is that it does not apply to all operators; we elaborate on this criteria in §5.4.

5.3 Case Study: Neighbors Within Range

We show the usage of provable quantization in TOD on neighbors within range (`NWR`, one of the FOs of our programming model), a common step in many OD algorithms, e.g., LOF [19] and LOCI [75]. `NWR` identifies nearest neighbors within a preset distance threshold (usually a small number), which may be considered as a variant of k nearest neighbors. More formally, given an input tensor $\mathbf{X} \coloneqq [X_1, X_2, ..., X_n] \in \mathbb{R}^{n\times d}$ (n samples and d dimensions) and the distance threshold ϕ, `NWR` first calculates the pairwise distance among each sample via the `cdist` operator, yielding a distance matrix $\mathbf{D} \in \mathbb{R}^{n\times n}$, where $\mathbf{D}_{i,j}$ is the pairwise distance between X_i and X_j. Then, each pairwise distance in $\mathbf{D}$ is compared with ϕ, and `NWR` outputs the indices of samples where $\mathbf{D}_{i,j} \le \phi$. As the pairwise distance calculation in `NWR` requires $O(n^2)$ space, provable quantization can provide significant GPU memory savings.

`NWR` meets the criterion we outline in §5.2, where eq. (2) can be applied to estimate the rounding errors. Recall that the pairwise Euclidean distance between two samples is

$$\mathbf{D}_{ij} = \left\|X_i - X_j\right\|_2^2 = \|X_i\|_2^2 + \left\|X_j\right\|_2^2 - 2X_i^T X_j. \tag{3}$$

We shall compute this in floating-point. Importantly, in our analysis to follow, the ordering of floating-point operations matters in determining rounding errors. To this end, we calculate distance using the right-most expression in eq. (3) (note that we do *not* first compute the difference $X_i - X_j$ and then compute its squared Euclidean norm). When calculating the first term in the RHS of eq. (3) via floating-point operations, we get

$$\begin{aligned}\mathrm{fl}(\|X_i\|_2^2) &= (X_{i,1} \otimes X_{i,1}) \oplus (X_{i,2} \otimes X_{i,2}) \oplus \cdots \oplus (X_{i,d} \otimes X_{i,d}) \\ &= (X_{i,1}^2(1+\delta_1)) \oplus (X_{i,2}^2(1+\delta_2)) \oplus \cdots \oplus (X_{i,d}^2(1+\delta_d)),\end{aligned}$$

where the second equality uses eq. (2) and we note that the errors $\delta_1, \ldots, \delta_d$ across the floating-point multiplications (for squaring) need not be the same (in fact, these need not be the same across samples $i = 1, 2, \ldots, n$ but we omit this indexing to keep the equation from getting cluttered).

Next, by defining $x_{\max} \triangleq \max_{i\in\{1,\ldots,n\},k\in\{1,\ldots,d\}} |X_{i,k}|$ and recalling from Theorem 1 that each of $\delta_1, \delta_2, \ldots, \delta_d$ above is at most ϵ, we get

$$\begin{aligned}\mathrm{fl}(\|X_i\|_2^2) &= (X_{i,1}^2(1+\delta_1)) \oplus (X_{i,2}^2(1+\delta_2)) \oplus \cdots \oplus (X_{i,d}^2(1+\delta_d)) \\ &\le \underbrace{[x_{\max}^2(1+\epsilon)] \oplus [x_{\max}^2(1+\epsilon)] \oplus \cdots \oplus [x_{\max}^2(1+\epsilon)]}_{d \text{ terms added via floating-point addition}} \\ &\le d \cdot x_{\max}^2(1+\epsilon)^{1+\lceil\log_2 d\rceil},\end{aligned}$$

where for the last step, $\log_2 d$ shows up since summation of d elements in lower-level programming languages is implemented in a divide-and-conquer manner that reduces to $\lceil\log_2 d\rceil$ operations (there is still a "1+" term in the exponent for the floating-point multiplication/squaring). The rounding error is bounded as follows:

$$\begin{aligned}\mathrm{Err}(\|X_i\|_2^2) &= \|X_i\|_2^2 - \mathrm{fl}(\|X_i\|_2^2) \\ &\le d \cdot x_{\max}^2 - \mathrm{fl}(\|X_i\|_2^2) \\ &\le \left|d \cdot x_{\max}^2 - \mathrm{fl}(\|X_i\|_2^2)\right| \\ &\le d \cdot x_{\max}^2[(1+\epsilon)^{1+\lceil\log_2 d\rceil} - 1].\end{aligned}$$

This same analysis can be used to bound the floating-point errors of the other terms in eq. (3). Overall, we get

$$\mathrm{Err}(\mathbf{D}_{ij}) \le 4d \cdot x_{\max}^2[(1+\epsilon)^{1+\lceil\log_2 d\rceil+2} - 1], \tag{4}$$

where the "+2" shows up in the exponent due to the addition and subtraction in the RHS of (3) that we compute in floating-point.

Inequality (4) provides a numerical way for checking whether a single entry $\mathbf{D}_{ij}$ is within the range of ϕ as $|\mathbf{D}_{ij} - \phi| > \mathrm{Err}(\mathbf{D}_{ij})$. More conveniently, we could scale the input $\mathbf{X}$ into the range of $[0, 1]$ before the distance calculation [79], so that $x_{\max} \le 1$ and the implementation complexity can be further reduced. With this treatment, a large amount of GPU memory can be saved in `NWR` operations (see §7.5 for results).

5.4 Applicability and Opportunities of Provable Quantization

Not all operators can benefit from provable quantization. To benefit from provable quantization, an operator needs to satisfy two criteria. First, the operator's output values cannot require a floating-point representation in the original precision, otherwise the exactness verification would require executing the operator in the original precision, resulting in no memory or time savings. For example, provable quantization is not applicable to `cdist` since its outputs are raw floating-point pairwise distances, and verifying its exactness requires calculating `cdist` in the original precision. Second, the performance gain in low-precision evaluation of the operator needs to be larger than the overhead of verification. Based on these two criteria, we mark the operators generally applicable for provable quantization by ★ in Fig. 2. Also see §7.5 for experimental results on this. Although the design of provable quantization is motivated by unsupervised OD algorithms with extensive ranking and selecting operations, other ML algorithms can also benefit if they meet the above criteria. For OD algorithms in which provable quantization does not apply, they could still benefit from TOD's other optimizations such as automatic batching (§6).

6 AUTOMATIC BATCHING AND MULTI-GPU SUPPORT

Motivation. Unlike CPU nodes with up to terabytes of DRAM, today's GPU nodes face much more stringent memory limitations [30, 49, 65, 66]—modern GPUs are mostly equipped with 4-40 GB of on-device memory [63, 87]. Out-of-memory (OOM) errors have thus become common in GPU-based systems for machine learning tasks [29]. To overcome this challenge, we design an *automatic batching* mechanism to decompose memory-intensive BTOs into multiple batches, which are executed on GPUs in a pipeline fashion. Automatic batching also allows TOD to equally distribute OD computation across multiple GPUs. TOD applies different mechanisms to decompose an operator into batches based on its data dependency. Specifically, an operator has *inter-sample dependency* if the computation of each sample requires accessing other samples, such as `cdist`. On the other hand, an operator has *inter-feature dependency* if the computation of each feature depends on other features, such as `Feat. sampler`. Fig. 4 summarizes TOD batching mechanisms for operators with and without these dependencies.

Direct batching. TOD automatically decomposes an operator into small batches if the operator is: (*i*) *sample-independent*: the estimation of each sample is independent, or (*ii*) *feature-independent*: the contribution of each feature is independent. When either condition holds, TOD directly partitions the operator into multiple batches by splitting along the sample or feature dimension, computes these batches in a pipeline fashion, and aggregates individual batches to produce the final output, as shown in Fig. 5. For instance, `topk` is a sample-independent operator. For an input tensor $\mathbf{X} \in \mathbb{R}^{n \times d}$, `topk` outputs the indices of the largest k values for each sample (i.e., row), resulting in an output tensor $\mathbf{I}_\mathbf{X} := \texttt{topk}(\mathbf{X}, k) \in \mathbb{R}^{n \times k}$. Therefore, we could split $\mathbf{X}$ into batches with full features, each with b samples (i.e.,, $\{\mathbf{X}_1, \mathbf{X}_2, ...\} \in \mathbb{R}^{b \times d}$). As another example, `Histogram` outputs the frequencies of each feature's values, which is feature-independent. Thus, we could partition $\mathbf{X}$ into blocks of b features, e.g., $\{\mathbf{X}_1, \mathbf{X}_2, ...\} \in \mathbb{R}^{n \times b}$.

Customized batching. For operators with *both* inter-sample and inter-feature dependencies, the computation of each data point involves all samples and features, and therefore cannot be directly decomposed into batches along the same or feature dimension. TOD provides customized batching strategies for these operators. For example, to automatically batch `cdist`, TOD uses the approach introduced in Neeb and Kurrus [69], which splits an input dataset across samples and calculates the pairwise distance of *each pair of split* in batches.

6.1 Sequential Batching and Operator Fusion

Simple concatenation. Since BTOs are independent from each other, executing a sequence of BTOs in batches is straightforward, i.e., simply feed the output of a batch operator as an input to another one. For example, *k*`NN` (see Fig. 2) finds the k nearest neighbors by first calculating pairwise distances of input samples via the `cdist` BTO and then returns the index of k items with the smallest distance via the `topk` BTO. Thus, *k*`NN` batching is achieved by running `cdist` and `topk` sequentially, where each uses automatic batching and the output of the former is the input of the latter. Note that simple concatenation applies to all BTOs and FOs as the default choice.

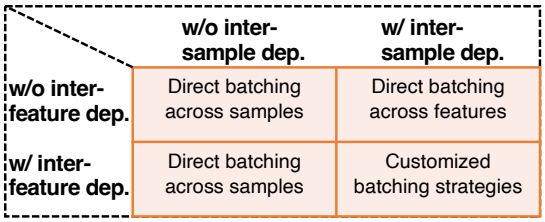

Figure 4: TOD applies automatic batching to operators without inter-sample or inter-feature dependency, and uses customized batching strategies for operators with both data dependencies.

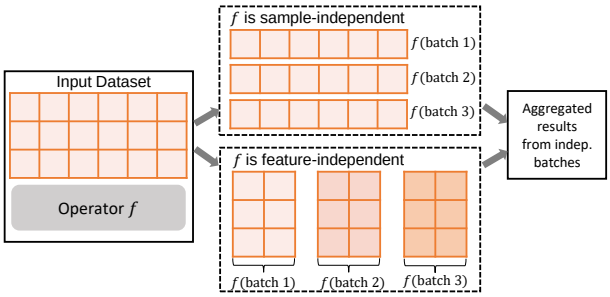

Figure 5: Direct batching with independence assumption creates batches along the sample or feature index.

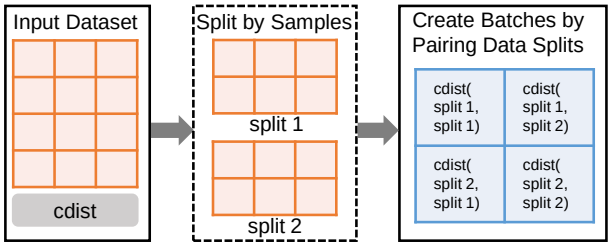

Figure 6: Customized batching solution for cdist in TOD.

Operator fusion. Although the simple concatenation discussed above is straightforward, a closer look unlocks deeper optimization opportunities in automatic batching with a sequence of operators. Notably, the output of *k*`NN` is the indices of the k nearest neighbors of an input dataset, where the pairwise distance generated by `cdist` is only used in an intermediate step but not returned. If we could prevent moving this large distance matrix between operators (i.e., `cdist` and `topk`), space efficiency can be improved. In deep learning systems, *operator fusion* is a common optimization technique to fuse multiple operators into a single one in a computational graph [15, 60, 64, 70, 93]. Fig. 7 compares simple concatenation (subfigure a) and operator fusion (subfigure b) on *k*`NN`. Specifically, the latter executes the `topk` BTO on the `cdist` BTO's individual batches separately rather than running `topk` on the full distance matrix outputted by `cdist`. Note that the global k nearest neighbors (of the full dataset) can be identified from the k local neighbor candidates from batches in the final aggregation, so the result is still exact. This prevents moving the entire $n \times n$ distance matrix between operators, which often causes OOM. TOD uses a *rule-based* approach to opportunistically fusing operators to reduce the kernel launch overhead and data transfers between CPUs and GPUs. TOD provides an interface that allows users to

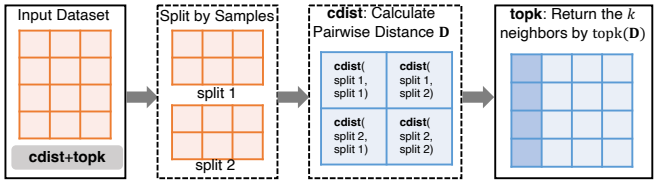

(a) Simple concatenation: `topk` is invoked on the full result of `cdist`—we need to communicate the large distance matrix D.

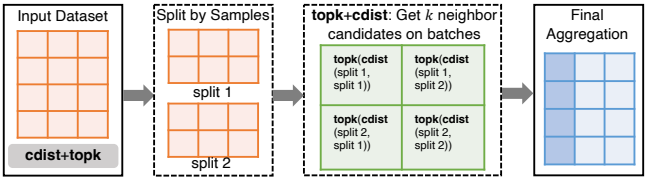

(b) Operator fusion: `topk` is directly invoked on the batch result of `cdsit`, preventing the communication of distance matrix D.

Figure 7: The comparison of automatic batching for kNN between simple concatenation and operator fusion. The latter has better scalability by not creating and moving large distance matrix D.

add fusion rules for new OD operators. Appx. C.3 provides a case study on the effectiveness of operator fusion.

6.2 Multi-GPU Support

To further reduce the execution time of OD algorithms on GPUs, TOD also supports multi-GPU execution, which is important for time-critical OD applications and has been widely used for other data-intensive applications such as graph neural networks [38]. Intuitively, if there is only one GPU, TOD iterates across multiple batches sequentially and aggregates the results. When multiple GPUs are available, we could achieve better performance by executing OD computations concurrently on multiple homogeneous GPUs. Specifically, TOD first applies automatic batching to an underlying task—multiple subtasks are created and assigned to available GPUs. TOD creates a *subprocess* for each available GPU to execute the assigned subtasks and a *shared global container* to store the results returned from each GPU. Since we equally distribute subtasks across GPUs, we deem the runtime of each GPU is close. Once all the subtasks are complete, the final output is generated by aggregating the results in the global container. For example, automatically batching `cdist` in Fig. 6 leads to 4 subtasks, each of which calculates the pairwise distances for a pair of splits (denoted as blue blocks in the figure). Each of the four available GPUs executes an assigned subtask and sends the `cdist` results to the global container. Finally, the full `cdist` result is obtained by aggregating the intermediate results in the global container. Note that the multi-GPU execution is at the operator level (e.g., `cdist`). §7.7 evaluates TOD's scalability across multiple GPUs.

7 EXPERIMENTAL EVALUATION

Our experiments answer the following questions:

(1) Is TOD more efficient (in time and space) than SOTA *CPU-based* OD system (i.e., PyOD) and selected *GPU* baselines? (§7.3)
(2) How scalable is TOD while handling more and more data? (§7.4)
(3) How effective are provable quantization and automatic batching), in comparison to PyTorch implementation? (§7.5 & 7.6)
(4) How much performance gain can TOD achieve on the multiple GPUs? (§7.7)

7.1 Implementation and Environment

TOD is implemented on top of PyTorch [76]. We extend PyTorch in the following aspects to support efficient OD. First, we implement a set of BTOs and FOs (see Fig. 2) for fast tensor operations in OD. Second, for operators that support provable quantization (see §5) and batching (see §6), we create corresponding versions of them to improve scalability. Additionally, we enable specialized multi-GPU support in TOD by leveraging PyTorch's `multiprocessing`. The usage and APIs of the open-sourced system can be found in §D.

Adding new operators . In addition to the BTOs and FOs listed in Fig. 2, users can add new operators in TOD by defining the operator's interface (i.e., the input and output tensors of the operator) and providing an implementation of the operator in PyTorch. This implementation will be used by TOD to decompose the operator into PyTorch's tensor algebra primitives and execute these primitives in parallel on multiple GPUs. For operators that do not have inter-sample *or* inter-feature dependency (see §6), TOD automatically decomposes the operator's computation into multiple batches. For operators that involve both inter-sample *and* inter-feature dependencies, TOD require users to provide a customized strategy to decompose the operator into batches.

Implementing new OD algorithms . One notable characteristic of OD is that most algorithms involve only straightforward computation, which can be decomposed into 2-3 BTOs and FOs. Therefore, we expect that implementing new OD algorithms in TOD should only involve low cognitive complexity. Appx. A demonstrates an implementation of a recent ECOD [53] detection algorithm in TOD in less than ten lines of code.

Experimental setup. All the experiments were performed on an Amazon EC2 cluster with an Intel Xeon E5-2686 v4 CPU, 61GB DRAM, and an NVIDIA Tesla V100 GPU. For the multi-GPU support evaluation, we extend it to multiple NVIDIA Tesla V100 GPUs with the same CPU node.

7.2 Datasets, Baselines, and Evaluation Metrics

Datasets. Table 2 shows the 11 real-world benchmark datasets used in this study, which are widely evaluated in OD research [21, 52, 82, 104] and available in the latest ADBench[1] [33]. Given the limited size of real-world OD datasets, we also build data generation function in TOD to create larger synthetic datasets (up to 1.5 million samples) to evaluate the scalability of TOD (see §7.4 for details).

OD algorithms and operators. Throughout the experiments, we compare the performance of five representative but diverse OD algorithms across different systems (see §2.1): proximity-based algorithms including LOF [19], ABOD [43], and kNN [10]; statistical method HBOS [31], and linear model PCA [85]. We also provide an operator-level analysis on selected BTOs and FOs to demonstrate the effectiveness of certain techniques.

Evaluation metrics. Since TOD and the baselines do not involve any approximation, the output results are exact and consistent

[1]Datasets available at ADBench: https://github.com/Minqi824/ADBench

Table 2: Real-world OD datasets used in the experiments. To demonstrate the results on larger datasets, we also create and use synthetic datasets throughout the experiments.

Dataset	Pts (n)	Dim (d)	% Outlier
musk	3,062	166	3.17
speech	3,686	400	1.65
mnist	7,603	100	9.21
mammography	11,183	6	2.32
ALOI	49,534	27	3.04
fashion-mnist	60,000	784	10
cifar-10	60,000	3072	10
celeba	202,599	39	2.24
fraud	284,807	29	0.17
census	299,285	500	6.20
donors	619,326	10	5.93

across systems. Therefore, we omit the accuracy evaluation, and compare the wall-clock time and GPU memory consumption as measures of time and space efficiency.

Baselines. As discussed in Section 2, there is no existing GPU system that covers a diverse group of OD algorithms (not even the above five algorithms) for a fair comparison. Therefore, we use the SOTA comprehensive system PyOD [105] as a *CPU* baseline in §7.3 and 7.4, which is deeply optimized with JIT compilation and parallelization. Regarding *GPU* baselines, we compare two representative OD algorithms (i.e., *k*NN-CUDA [9] and LOF-CUDA [6]) that have GPU support in §7.3, and direct implementation of operators in PyTorch in §7.5, 7.6, and 7.7. Note that the implementation of *k*NN-CUDA and LOF-CUDA are not open-sourced, so we follow the original papers to implement.

7.3 End-to-end Evaluation

TOD **is significantly faster than the leading CPU-based system**. We first present the runtime comparison between TOD and PyOD in Fig. 8 using seven real datasets (ALOI, fashion-mnist, and cifar-10) and Appx. Fig. C3 with three synthetic datasets (where Synthetic 1 contains 100,000 samples, Synthetic 2 contains 200,000 samples, and Synthetic 3 contains 400,000 samples (all are with 200 features). The results show that TOD is on average 10.9× faster than PyOD on the five benchmark algorithms (13.0×, 15.9×, 9.3×, 7.2×, and 8.9× speed-up on LOF, *k*NN, ABOD, HBOS, and PCA, respectively). For proximity-based algorithms, a larger speed-up is observed for datasets with a higher number of dimensions: LOF and *k*NN are 28.1× and 38.9× faster on cifar-10 with 3,072 features. This is expected as GPUs are well-suited for dense tensor multiplication, which is essential in proximity-based methods. Separately, a larger improvement can be achieved for HBOS and PCA on datasets with larger sample sizes. For instance, HBOS is 11.83× faster on Synthetic 1 (100,000 samples), while the speedup is 17.16× on Synthetic 2 (200,000 samples). This is expected as HBOS treats each feature independently for density estimation on GPUs, so a large number of samples with a small number of features should yield a significant speed-up. In summary, all the OD algorithms tested are significantly faster in TOD than in the SOTA PyOD system,

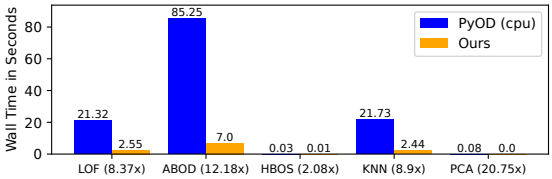

(a) ALOI (49,534 samples with 27 features)

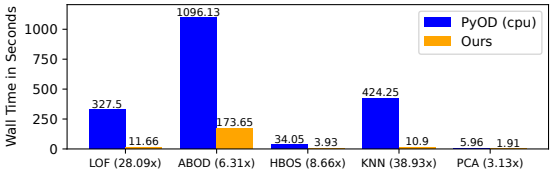

(b) cifar-10 (60,000 samples with 784 features)

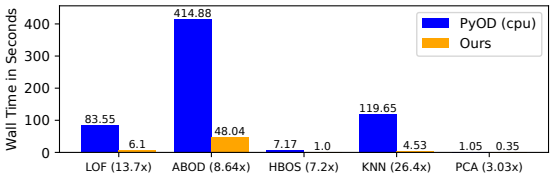

(c) fashion-mnist (60,000 samples with 3,072 features)

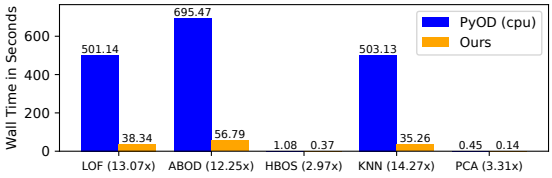

(d) celeba (202,599 samples with 39 features)

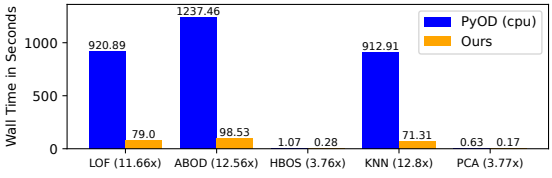

(e) fraud (284,807 samples with 29 features)

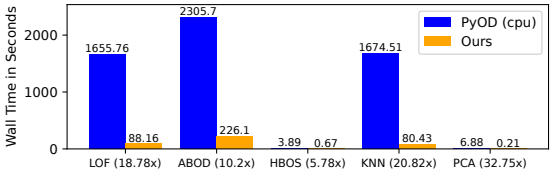

(f) census (299,285 samples with 500 features)

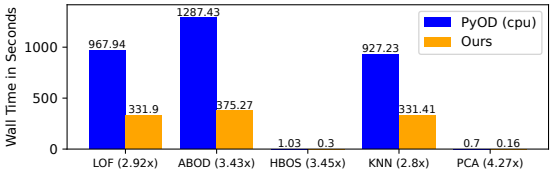

(g) donors (619,326 samples with 10 features)

Figure 8: Runtime comparison between PyOD and TOD **in seconds on both real-world and synthetic datasets (see Appx. Fig C3 for synthetic data results).** TOD **significantly outperforms PyOD in all w/ much smaller runtime, where the speedup factor is shown in parenthesis by each algorithm. On avg.,** TOD **is 10.9× faster than PyOD (up to 38.9×).**

Table 3: Runtime comparison among selected GPU baselines (*k*NN-CUDA [9] and LOF-CUDA [6]; neither supports multi-GPU directly), and TOD (single GPU) and TOD-8 (8 GPUs). The first column shows three synthetic datasets with an increasing number of samples (100 dimensions), and the most efficient result is highlighted in bold for each setting. TOD-8 outperforms in all cases due to multi-GPU support, while TOD with a single GPU is faster or on par with the baselines. Note that the GPU baselines run out-of-memory (OOM) on large datasets (e.g., the last row), while TOD does not.

Dataset	*k*NN-CUDA	TOD	TOD-8	LOF-CUDA	TOD	TOD-8
500,000	205.33	208.84	**28.59**	312.55	209	**28.64**
1,000,000	850.12	827	**112.35**	OOM	819	**113.72**
2,000,000	OOM	3173.39	**430.29**	OOM	3174.05	**434.18**

with the precise amount of speed improvement varying across algorithms. Appx. C.2 shows that GPU computation takes most of the run time for various OD algorithms, explaining the significant time reduction by TOD. We also provide ablation studies to evaluate provable quantization and automatic batching in Appx. C.4.

TOD **can handle larger datasets than the GPU baselines**. Due to the absence of GPU systems that support all five OD algorithms, we specifically compare the performance of TOD to specialized GPU algorithms *k*NN-CUDA [9] and LOF-CUDA [6]. Table 3 shows that TOD with 8-GPUs outperforms in all three datasets due to the multi-GPU support, which enables it to handle data more efficient than the baselines and TOD with a single GPU. By focusing on the use of a single GPU, we find that TOD is faster or on par with both baselines due to provable quantization (e.g., 33.13% speedup to LOF-CUDA). Also note that the GPU baselines face the out-of-memory issue (OOM) on large datasets (e.g., the last row of the table with 2,000,000 samples), while TOD can still handle it due to automatic batching. In comparison to these specialized GPU baselines, TOD does not only provide more coverage of diverse algorithms, but also yields better efficiency and scalability.

7.4 Scalability of TOD

We now gauge the scalability of TOD on datasets of varying sizes, including ones larger than fashion-mnist and cifar-10. In Fig. 9, we plot TOD's runtime with five OD algorithms on the synthetic datasets with sample sizes ranging from 50,000 to 1,500,000 (all with 200 features). To the best of our knowledge, none of the existing comprehensive OD systems can handle datasets with more than a million samples within a reasonable amount of time [4, 103], as most of the OD algorithms are associated with quadratic time complexity. Fig. 9 shows that TOD can process million-sample OD datasets within an hour, providing a scalable approach to deploying OD algorithms in many real-world tasks.

7.5 Provable Quantization

Provable quantization (§5) in TOD can optimize the operator memory usage while provably preserving correctness (i.e., no accuracy degradation). To demonstrate its effectiveness, we compare the GPU memory consumption of two applicable operators, `nwr` and `topk`, with and without provable quantization using the GPU baseline.

Table 4: Comparison of operator runtime (in seconds) with provable quantization (i.e., 16-bit and 32-bit) and without quantization (i.e., 64-bit) for `nwr` and `topk`. The best model is highlighted in bold (per column), where provable quantization in 16-bit outperforms the rest in most cases.

Prec.	mammog.	mnist	musk	10k	20k	30k
16-bit	**2.66**	**0.54**	**0.06**	**0.87**	**3.02**	**6.56**
32-bit	2.92	1.51	0.09	2.57	10.09	22.51
64-bit	3.31	1.53	0.09	3.49	12.7	27.32

(a) For `nwr`, 16-bit provable quantization outperforms in all

Prec.	cifar-10	f-mnist	speech	1M	2M	5M
16-bit	**0.31**	0.09	0.0054	**0.58**	**1.16**	**2.90**
32-bit	0.32	0.1	0.0048	0.70	1.40	3.52
64-bit	0.34	**0.07**	**0.0038**	0.71	1.73	3.88

(b) For `topk`, 16-bit provable quantization wins for large data

Multiple real-world and synthetic datasets are used in the comparison (see Table 2), where synthetic datasets' names, such as "10k" and "1M", denote their sample sizes. We deem the 64-bit floating point as the ground truth, and evaluate the provable quantization results in 32- and 16-bit floating-point.

The results demonstrate that provable quantization always leads to memory savings. Specifically, Fig. 10 (a-b) shows `nwr` with provable quantization on average saves 71.27% (with 16-bit precision) and 47.59% (with 32-bit precision) of the full 64-bit precision GPU memory. Similarly, Fig. 10 (c-d) shows that `topk` with provable quantization saves 73.49% (with 16-bit precision) and 49.58% (with 32-bit precision) of the full precision memory. Regarding the runtime comparison, operating in lower precision may also lead to an edge. Table 4 shows the operator runtime comparison between using provable quantization (in 16-bit and 32-bit precision) and using the full 64-bit precision. It shows that provable quantization in 16-bit precision is faster than the computations in full precision in most cases, especially for large datasets (e.g., the last three columns of Table 4). This empirical finding can be attributed to lower-precision operations typically being faster, and this speed improvement outweighs the overhead of post verification (see §5.4). For small datasets (the first three columns of Table 4), provable quantization does not necessarily improve the run time due to the additional verification and data movement, both of which finish in 0.1 seconds.

Case study on runtime breakdown . In addition to comparing the total runtime of an operator with or without provable quantization (§7.5), it is interesting to see the time breakdown of each phase of provable quantization. Specifically, the runtime of provable quantization can be divided into (*i*) operator evaluation in lower precision, (*ii*) result verification and (*iii*) recalculation in the original precision for the ones that fail in the verification. Taking `nwr` on 30k samples as an example (the last column of Table 4a), we show the time breakdown of (*i*) low-precision evaluation (*ii*) correctness verification and (*iii*) recalculation in higher precision in Table 5. In this case, the performance improvement of provable quantization comes from the reduced evaluation time in lower precision, which outweighs

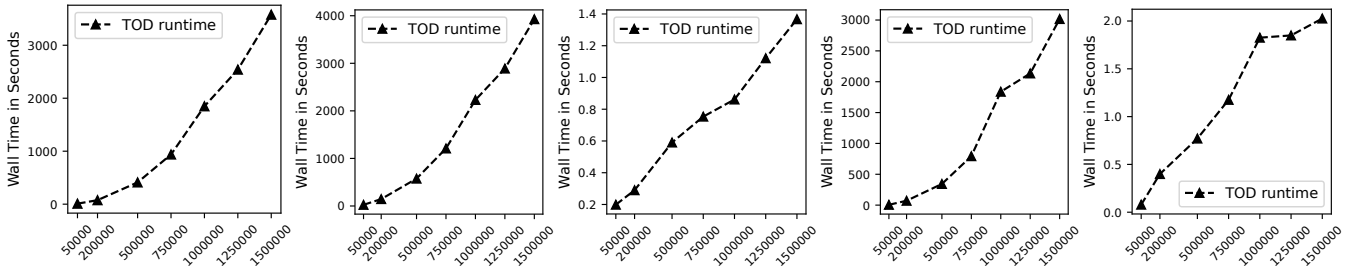

(a) LOF (quadratic) (b) ABOD (quadratic) (c) HBOS (linear) (d) kNN (quadratic) (e) PCA (linear)

Figure 9: Scalability plot of selected algorithms in TOD, where it scales well with an increasing number of samples.

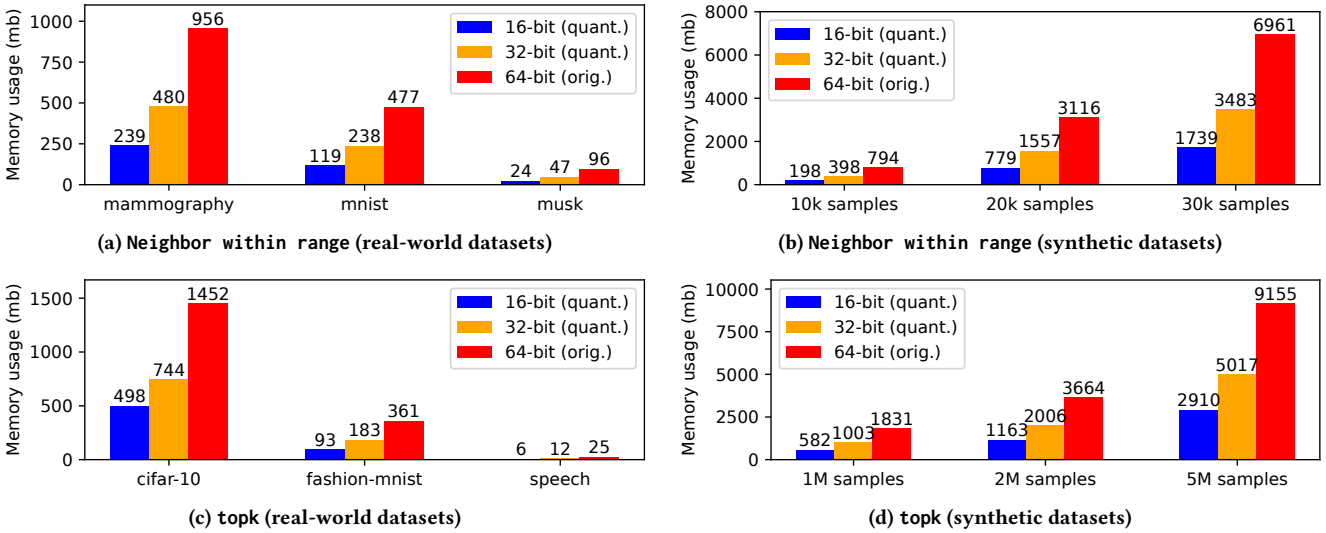

(a) `Neighbor within range` (real-world datasets)

(b) `Neighbor within range` (synthetic datasets)

(c) `topk` (real-world datasets)

(d) `topk` (synthetic datasets)

Figure 10: GPU memory consumption comparison between using provable quantization (16-bit and 32-bit) and the full precision (64-bit). Clearly, provable quantization leads to significant memory consumption saving on `nwr` and `topk`.

Table 5: Runtime breakdown of using provable quantization on `nwr` operator with a 30,000 sample synthetic dataset. Column 1 shows the runtime for low-precision evaluation, where column 2 and 3 show the runtime for correctness verification and recalculation, respectively. It shows the primary speed-up comes from low-precision evaluation, while the overhead of verification and recalculation is marginal.

Prec.	Low Prec.	Verification	Recalculation	Total
16-bit	5.91	0.05	0.61	6.56
32-bit	22	0.05	0.47	22.51
64-bit	N/A	N/A	N/A	27.32

the cost of verification and recalculation. To further demonstrate the necessity of post-verification, we also measure the accuracy variation (e.g., ROC-AUC [4]) by simply running kNN detector on fraud, census, and donors datasets in 16-bit precision without post-verification, which leads to −3.48%, +1.05%, −4.27% accuracy variation. These results show the merit of provable quantization over direct quantization.

7.6 Automatic Batching

To evaluate the effectiveness of automatic batching, we compare the runtime of multiple BOs and FOs under (*i*) an Numpy implementation on a CPU [34], (*ii*) a direct PyTorch GPU implementation without batching [76], and (*iii*) TOD's automatic batching.

Table 6 compares the three implementations of key operators in OD systems. Clearly, TOD with automatic batching achieves the best balance of efficiency and scalability, leading to 7.22×, 17.46×, and 11.49× speedups compared to a highly optimized NumPy implementation on CPUs. TOD can also handle more than 10× larger datasets where the direct PyTorch implementation faces out of memory (OOM) errors. TOD is only marginally slower than PyTorch when the input dataset is small (see the first row of each operator). In this case, batching is not needed, and TOD is equivalent to PyTorch; TOD is slightly slower due to the overhead of TOD deciding whether or not to enable automatic batching.

7.7 Multi-GPU Results

We now evaluate the scalability of TOD on multiple GPUs on a single compute node. Specifically, we compare the run time of three compute-intensive OD algorithms (i.e., LOF, ABOD, and kNN) with 1,2,4, and 8 NVIDIA Tesla V100 GPUs.

Table 6: Operator runtime comparison among implementations in NumPy (no batching), PyTorch (no batching) and TOD **(with automatic batching); the most efficient result is highlighted in bold per row. Automatic batching in** TOD **prevents out-of-memory (OOM) errors yet shows great efficiency, especially on large datasets.**

Operator	Size	NumPy	PyTorch	TOD
topk	10,000,000	7.88	**1.08**	1.09
topk	20,000,000	15.77	OOM	**2.44**
topk	100,000,000	OOM	OOM	**10.83**
intersect	20,000,000	1.99	**0.12**	0.14
intersect	100,000,000	11	**0.63**	**0.63**
intersect	200,000,000	21.65	OOM	**2.11**
*k*NN	50,000	20.15	**0.27**	0.28
*k*NN	200,000	194.43	OOM	**19.65**
*k*NN	400,000	818.32	OOM	**71.22**

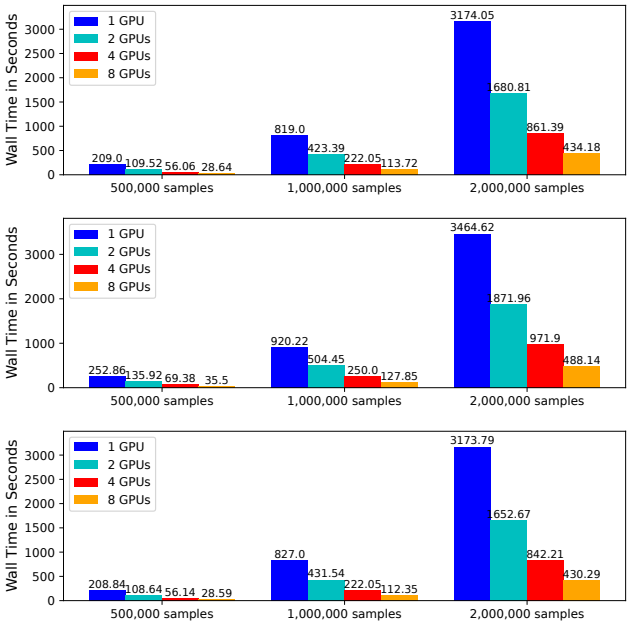

Figure 11: Runtime comparison of using different numbers of GPUs (top: LOF; middle: ABOD; bottom: *k*NN). TOD **can efficiently leverage multiple GPUs for faster OD.**

Fig. 11 shows that for three OD algorithms tested, TOD can achieve nearly linear speed-up with more GPUs—the GPU efficiency is mostly above 90%. For instance, the *k*NN result shows that using 2, 4, and 8 GPUs are 1.91×, 3.73×, and 7.34× faster than the single-GPU performance. As a comparison, using 2, 4, and 8 GPUs with ABOD and LOF are 1.85×, 3.63×, 7.14× faster and 1.91×, 3.70×, 7.27× faster, respectively. First, there is inevitably a small overhead in multi-processing, causing the speed-up to not exactly be linear. Second, the minor efficiency difference between *k*NN and ABOD is due to most OD operations in the former being executed on multiple GPUs, while the latter involves several sequential steps that have to be run on CPUs. To sum up, TOD can leverage multiple GPUs efficiently to process large datasets.

8 LIMITATIONS AND FUTURE DIRECTIONS

Tree-based OD algorithms. One limitation of TOD is that it does not support tree-based OD algorithms such as isolation forests [55]. Tree-based operations involve random data access [51], which is not friendly for GPUs designed for batch operations. Future work can consider converting trees to tensor operations [67] for acceleration.

Approximate solutions. Our focus in this paper has been on *exact* efficient, scalable implementations of OD algorithms. In particular, we have not considered implementations that intentionally are meant to be approximate, where for instance, one could trade off between accuracy, computation time, and memory usage. Note that even with our provable quantization technique, we ask for the lower-precision computation to yield the correct (exact) output. A future research direction is to extend TOD to support approximate solutions for even better scalability and efficiency when reduced accuracy is acceptable. For instance, exact nearest neighbor search in can be switched to approximate nearest neighbor search [27, 94].

Heterogeneous GPUs. Thus far, we have not studied the use of TOD with heterogeneous GPUs. In this setting, incorporating a cost model could be helpful in balancing the workload between the different GPUs, accounting for their different characteristics such as varying memory capacities.

Gradient-based operators. Currently, TOD does not support operators that involve solving an optimization problem via gradient descent. Future work may consider incorporating optimization-based operators to support (a small group of) optimization-based OD algorithms, e.g., OCSVM [83].

Extension to classification. It is possible to use TOD to build classification models, as the operators in TOD are generic and may serve the tasks beyond OD. We provide an example of using TOD to construct k nearest neighbor classifier in Appx. B, which also exhibits a significant performance improvement over the CPU implementation in scikit-learn [77]. Note that classification tasks often involve optimization (e.g., via gradient descent), which we already pointed out that TOD does not yet support. Thus, only calculation-based classifiers can be implemented by TOD for now.

9 CONCLUSION

In this paper, we propose the first comprehensive GPU-based outlier detection system called TOD, which is on average 10.9 times faster than the leading system PyOD and is capable of handling larger datasets than existing GPU baselines. The key idea is to decompose complex outlier detection algorithms into a combination of tensor operations for effective GPU acceleration. Our system enables many large-scale real-world outlier detection applications that could have stringent time constraints. With the ease of extensibility, TOD can prototype and implement new detection algorithms.

ACKNOWLEDGEMENT

We would like to thank the anonymous reviewers for their helpful comments. Yue Zhao is partially supported by a Norton Graduate Fellowship. George H. Chen is supported by NSF CAREER award #2047981. Zhihao Jia is partially supported by an Amazon research award, a Google faculty award, a Meta research award, a Tang family endowment, and NSF awards CNS-2147909 and CNS-2211882.

REFERENCES

[1] Martín Abadi, Paul Barham, Jianmin Chen, Zhifeng Chen, Andy Davis, Jeffrey Dean, Matthieu Devin, Sanjay Ghemawat, Geoffrey Irving, Michael Isard, Manjunath Kudlur, Josh Levenberg, Rajat Monga, Sherry Moore, Derek Gordon Murray, Benoit Steiner, Paul A. Tucker, Vijay Vasudevan, Pete Warden, Martin Wicke, Yuan Yu, and Xiaoqiang Zheng. 2016. TensorFlow: A System for Large-Scale Machine Learning. In *12th USENIX Symposium on Operating Systems Design and Implementation, OSDI 2016, Savannah, GA, USA, November 2-4, 2016*, Kimberly Keeton and Timothy Roscoe (Eds.). USENIX Association, 265–283. https://www.usenix.org/conference/osdi16/technical-sessions/presentation/abadi

[2] Ahmed Abdulaal, Zhuanghua Liu, and Tomer Lancewicki. 2021. Practical approach to asynchronous multivariate time series anomaly detection and localization. In *Proceedings of the 27th ACM SIGKDD Conference on Knowledge Discovery & Data Mining*. ACM, 2485–2494.

[3] Elke Achtert, Hans-Peter Kriegel, Lisa Reichert, Erich Schubert, Remigius Wojdanowski, and Arthur Zimek. 2010. Visual Evaluation of Outlier Detection Models. In *Database Systems for Advanced Applications, 15th International Conference, DASFAA 2010, Tsukuba, Japan, April 1-4, 2010, Proceedings, Part II (Lecture Notes in Computer Science)*, Hiroyuki Kitagawa, Yoshiharu Ishikawa, Qing Li, and Chiemi Watanabe (Eds.), Vol. 5982. Springer, 396–399. https://doi.org/10.1007/978-3-642-12098-5_34

[4] Charu C. Aggarwal. 2013. *Outlier Analysis*. Springer.

[5] Charu C Aggarwal, Yuchen Zhao, and S Yu Philip. 2011. Outlier detection in graph streams. In *2011 IEEE 27th international conference on data engineering*. IEEE, IEEE, 399–409.

[6] Malak Alshawabkeh, Byunghyun Jang, and David R. Kaeli. 2010. Accelerating the local outlier factor algorithm on a GPU for intrusion detection systems. In *Proceedings of 3rd Workshop on General Purpose Processing on Graphics Processing Units, GPGPU 2010, Pittsburgh, Pennsylvania, USA, March 14, 2010 (ACM International Conference Proceeding Series)*, David R. Kaeli and Miriam Leeser (Eds.), Vol. 425. ACM, 104–110. https://doi.org/10.1145/1735688.1735707

[7] Fabien André, Anne-Marie Kermarrec, and Nicolas Le Scouarnec. 2016. Cache locality is not enough: High-performance nearest neighbor search with product quantization fast scan. In *VLDB*, Vol. 9. VLDB Endowment, 12.

[8] Fabrizio Angiulli, Stefano Basta, Stefano Lodi, and Claudio Sartori. 2010. A Distributed Approach to Detect Outliers in Very Large Data Sets. In *Euro-Par 2010 - Parallel Processing*. Springer Berlin Heidelberg, Berlin, Heidelberg, 329–340.

[9] Fabrizio Angiulli, Stefano Basta, Stefano Lodi, and Claudio Sartori. 2016. GPU Strategies for Distance-Based Outlier Detection. *IEEE Trans. Parallel Distributed Syst.* 27, 11 (2016), 3256–3268.

[10] Fabrizio Angiulli and Clara Pizzuti. 2002. Fast Outlier Detection in High Dimensional Spaces. In *Principles of Data Mining and Knowledge Discovery, 6th European Conference, PKDD 2002, Helsinki, Finland, August 19-23, 2002, Proceedings (Lecture Notes in Computer Science)*, Tapio Elomaa, Heikki Mannila, and Hannu Toivonen (Eds.), Vol. 2431. Springer, 15–26. https://doi.org/10.1007/3-540-45681-3_2

[11] Fadhel Ayed, Lorenzo Stella, Tim Januschowski, and Jan Gasthaus. 2020. Anomaly detection at scale: The case for deep distributional time series models. In *International Conference on Service-Oriented Computing*. Springer, 97–109.

[12] Fatemeh Azmandian, Ayse Yilmazer, Jennifer G. Dy, Javed A. Aslam, and David R. Kaeli. 2012. GPU-Accelerated Feature Selection for Outlier Detection Using the Local Kernel Density Ratio. In *12th IEEE International Conference on Data Mining, ICDM 2012, Brussels, Belgium, December 10-13, 2012*, Mohammed Javeed Zaki, Arno Siebes, Jeffrey Xu Yu, Bart Goethals, Geoffrey I. Webb, and Xindong Wu (Eds.). IEEE Computer Society, 51–60. https://doi.org/10.1109/ICDM.2012.51

[13] Kanishka Bhaduri, Bryan L Matthews, and Chris R Giannella. 2011. Algorithms for speeding up distance-based outlier detection. In *KDD*. ACM, 859–867.

[14] Davis W Blalock and John V Guttag. 2017. Bolt: Accelerated data mining with fast vector compression. In *KDD*. ACM, 727–735.

[15] Matthias Boehm, Berthold Reinwald, Dylan Hutchison, Prithviraj Sen, Alexandre V. Evfimievski, and Niketan Pansare. 2018. On Optimizing Operator Fusion Plans for Large-Scale Machine Learning in SystemML. *Proc. VLDB Endow.* 11, 12 (2018), 1755–1768. https://doi.org/10.14778/3229863.3229865

[16] Paul Boniol and Themis Palpanas. 2020. Series2graph: Graph-based subsequence anomaly detection for time series. *VLDB* 13, 12 (2020), 1821–1834.

[17] Paul Boniol, Themis Palpanas, Mohammed Meftah, and Emmanuel Remy. 2020. GraphAn: Graph-based subsequence anomaly detection. *VLDB* 13, 12 (2020), 2941–2944.

[18] Paul Boniol, John Paparrizos, Themis Palpanas, and Michael J Franklin. 2021. SAND: streaming subsequence anomaly detection. *VLDB* 14, 10 (2021), 1717–1729.

[19] Markus M. Breunig, Hans-Peter Kriegel, Raymond T. Ng, and Jörg Sander. 2000. LOF: Identifying Density-Based Local Outliers.. In *SIGMOD*. ACM, 93–104.

[20] Lars Buitinck, Gilles Louppe, Mathieu Blondel, Fabian Pedregosa, Andreas Mueller, Olivier Grisel, Vlad Niculae, Peter Prettenhofer, Alexandre Gramfort, Jaques Grobler, Robert Layton, Jake VanderPlas, Arnaud Joly, Brian Holt, and Gaël Varoquaux. 2013. API design for machine learning software: experiences from the scikit-learn project. In *Proceedings of ECML PKDD Workshop: Languages for Data Mining and Machine Learning*. ECML, 108–122.

[21] Guilherme O Campos, Arthur Zimek, Jörg Sander, Ricardo JGB Campello, Barbora Micenková, Erich Schubert, Ira Assent, and Michael E Houle. 2016. On the evaluation of unsupervised outlier detection: measures, datasets, and an empirical study. *Data mining and knowledge discovery* 30, 4 (2016), 891–927.

[22] Lei Cao, Qingyang Wang, and Elke A Rundensteiner. 2014. Interactive outlier exploration in big data streams. *VLDB* 7, 13 (2014), 1621–1624.

[23] Lei Cao, Yizhou Yan, Samuel Madden, Elke A Rundensteiner, and Mathan Gopalsamy. 2019. Efficient discovery of sequence outlier patterns. *VLDB* 12, 8 (2019), 920–932.

[24] Steve Dai, Rangharajan Venkatesan, Haoxing Ren, Brian Zimmer, William J. Dally, and Brucek Khailany. 2021. VS-Quant: Per-vector Scaled Quantization for Accurate Low-Precision Neural Network Inference. *CoRR* (2021). arXiv:2102.04503

[25] Jia Deng, Wei Dong, Richard Socher, Li-Jia Li, Kai Li, and Li Fei-Fei. 2009. Imagenet: A large-scale hierarchical image database. In *2009 IEEE conference on computer vision and pattern recognition*. IEEE, 248–255.

[26] Evelyn Fix and Joseph Lawson Hodges. 1989. Discriminatory analysis. Nonparametric discrimination: Consistency properties. *International Statistical Review/Revue Internationale de Statistique* 57, 3 (1989), 238–247.

[27] Cong Fu, Chao Xiang, Changxu Wang, and Deng Cai. 2019. Fast approximate nearest neighbor search with the navigating spreading-out graph. *VLDB* 12, 5 (2019), 461–474.

[28] Tianfan Fu, Cao Xiao, Cheng Qian, Lucas M Glass, and Jimeng Sun. 2021. Probabilistic and Dynamic Molecule-Disease Interaction Modeling for Drug Discovery. In *KDD*. ACM, 404–414.

[29] Yanjie Gao, Yu Liu, Hongyu Zhang, Zhengxian Li, Yonghao Zhu, Haoxiang Lin, and Mao Yang. 2020. Estimating GPU memory consumption of deep learning models. In *ESEC/FSE*. ACM, 1342–1352.

[30] Prasun Gera, Hyojong Kim, Piyush Sao, Hyesoon Kim, and David Bader. 2020. Traversing large graphs on GPUs with unified memory. *VLDB* 13, 7 (2020), 1119–1133.

[31] Markus Goldstein and Andreas Dengel. 2012. Histogram-based outlier score (hbos): A fast unsupervised anomaly detection algorithm. *KI* (2012), 59–63.

[32] Ian Goodfellow, Yoshua Bengio, and Aaron Courville. 2016. *Deep learning*. MIT.

[33] Songqiao Han, Xiyang Hu, Hailiang Huang, Mingqi Jiang, and Yue Zhao. 2022. ADBench: Anomaly Detection Benchmark. *arXiv preprint arXiv:2206.09426* (2022).

[34] Charles R Harris, K Jarrod Millman, Stéfan J van der Walt, Ralf Gommers, Pauli Virtanen, David Cournapeau, Eric Wieser, Julian Taylor, Sebastian Berg, Nathaniel J Smith, et al. 2020. Array programming with NumPy. *Nature* (2020).

[35] Kaiming He, Xiangyu Zhang, Shaoqing Ren, and Jian Sun. 2016. Deep residual learning for image recognition. In *Proceedings of the IEEE conference on computer vision and pattern recognition*. IEEE, 770–778.

[36] Vincent Jacob, Fei Song, Arnaud Stiegler, Bijan Rad, Yanlei Diao, and Nesime Tatbul. 2021. A demonstration of the exathlon benchmarking platform for explainable anomaly detection. *VLDB (PVLDB)* (2021).

[37] Zhuoran Ji and Cho-Li Wang. 2021. Accelerating DBSCAN Algorithm with AI Chips for Large Datasets. In *ICPP 2021: 50th International Conference on Parallel Processing, Lemont, IL, USA, August 9 - 12, 2021*, Xian-He Sun, Sameer Shende, Laxmikant V. Kalé, and Yong Chen (Eds.). ACM, 51:1–51:11. https://doi.org/10.1145/3472456.3473518

[38] Zhihao Jia, Sina Lin, Mingyu Gao, Matei Zaharia, and Alex Aiken. 2020. Improving the Accuracy, Scalability, and Performance of Graph Neural Networks with Roc. In *MLSys*. mlsys.org.

[39] Zhihao Jia, Matei Zaharia, and Alex Aiken. 2019. Beyond Data and Model Parallelism for Deep Neural Networks. In *Proceedings of Machine Learning and Systems 2019, MLSys 2019, Stanford, CA, USA, March 31 - April 2, 2019*, Ameet Talwalkar, Virginia Smith, and Matei Zaharia (Eds.). mlsys.org. https://proceedings.mlsys.org/book/265.pdf

[40] William Kahan. 1996. IEEE standard 754 for binary floating-point arithmetic. *Lecture Notes on the Status of IEEE* 754, 94720-1776 (1996), 11.

[41] Kyle Kingsbury and Peter Alvaro. 2020. Elle: inferring isolation anomalies from experimental observations. *VLDB* 14, 3 (2020), 268–280.

[42] Dimitrios Koutsoukos, Supun Nakandala, Konstantinos Karanasos, Karla Saur, Gustavo Alonso, and Matteo Interlandi. 2021. Tensors: An abstraction for general data processing. *VLDB* 14, 10 (2021), 1797–1804.

[43] Hans-Peter Kriegel, Matthias Schubert, and Arthur Zimek. 2008. Angle-based outlier detection in high-dimensional data.. In *KDD*. ACM, 444–452.

[44] Kwei-Herng Lai, Daochen Zha, Junjie Xu, Yue Zhao, Guanchu Wang, and Xia Hu. 2021. Revisiting Time Series Outlier Detection: Definitions and Benchmarks. In *Proceedings of the Neural Information Processing Systems Track on Datasets and Benchmarks 1, NeurIPS Datasets and Benchmarks 2021, December 2021, virtual*. Joaquin Vanschoren and Sai-Kit Yeung. https://datasets-benchmarks-proceedings.neurips.cc/paper/2021/hash/ec5decca5ed3d6b8079e2e7e7bacc9f2-Abstract-round1.html

[45] Aleksandar Lazarevic, Levent Ertöz, Vipin Kumar, Aysel Ozgur, and Jaideep Srivastava. 2003. A Comparative Study of Anomaly Detection Schemes in

Network Intrusion Detection. In *SDM*. SIAM, 25–36.
[46] Eleazar Leal and Le Gruenwald. 2018. Research Issues of Outlier Detection in Trajectory Streams Using GPUs. *SIGKDD Explor.* 20, 2 (2018), 13–20.
[47] Yann LeCun. 2019. 1.1 deep learning hardware: past, present, and future. In *2019 IEEE International Solid-State Circuits Conference-(ISSCC)*. IEEE, 12–19.
[48] Meng-Chieh Lee, Yue Zhao, Aluna Wang, Pierre Jinghong Liang, Leman Akoglu, Vincent S. Tseng, and Christos Faloutsos. 2020. AutoAudit: Mining Accounting and Time-Evolving Graphs. In *Big Data*. IEEE, 950–956.
[49] Rubao Lee, Minghong Zhou, Chi Li, Shenggang Hu, Jianping Teng, Dongyang Li, and Xiaodong Zhang. 2021. The art of balance: a RateupDB™ experience of building a CPU/GPU hybrid database product. *VLDB* 14, 12 (2021), 2999–3013.
[50] Wonyeol Lee, Rahul Sharma, and Alex Aiken. 2018. On automatically proving the correctness of math.h implementations. *Proc. ACM Program. Lang.* 2, POPL (2018), 47:1–47:32. https://doi.org/10.1145/3158135
[51] Aaron E Lefohn, Shubhabrata Sengupta, Joe Kniss, Robert Strzodka, and John D Owens. 2006. Glift: Generic, efficient, random-access GPU data structures. *ACM Transactions on Graphics (TOG)* 25, 1 (2006), 60–99.
[52] Zheng Li, Yue Zhao, Nicola Botta, Cezar Ionescu, and Xiyang Hu. 2020. COPOD: Copula-Based Outlier Detection. In *ICDM*. IEEE, 1118–1123.
[53] Zheng Li, Yue Zhao, Xiyang Hu, Nicola Botta, Cezar Ionescu, and George Chen. 2022. ECOD: Unsupervised Outlier Detection Using Empirical Cumulative Distribution Functions. *IEEE Transactions on Knowledge and Data Engineering* (2022), 1–1. https://doi.org/10.1109/TKDE.2022.3159580
[54] Can Liu, Li Sun, Xiang Ao, Jinghua Feng, Qing He, and Hao Yang. 2021. Intention-aware heterogeneous graph attention networks for fraud transactions detection. In *Proceedings of the 27th ACM SIGKDD Conference on Knowledge Discovery & Data Mining*. 3280–3288.
[55] Fei Tony Liu, Kai Ming Ting, and Zhi-Hua Zhou. 2008. Isolation Forest. In *ICDM*. IEEE Computer Society, 413–422.
[56] Haoyu Liu, Fenglong Ma, Shibo He, Jiming Chen, and Jing Gao. 2021. Fairness-aware Outlier Ensemble. *arXiv preprint arXiv:2103.09419* (2021).
[57] Kay Liu, Yingtong Dou, Yue Zhao, Xueying Ding, Xiyang Hu, Ruitong Zhang, Kaize Ding, Canyu Chen, Hao Peng, Kai Shu, et al. 2022. Benchmarking Node Outlier Detection on Graphs. *arXiv preprint arXiv:2206.10071* (2022).
[58] Kay Liu, Yingtong Dou, Yue Zhao, Xueying Ding, Xiyang Hu, Ruitong Zhang, Kaize Ding, Canyu Chen, Hao Peng, Kai Shu, et al. 2022. PyGOD: A Python Library for Graph Outlier Detection. *arXiv preprint arXiv:2204.12095* (2022).
[59] Zhiwei Liu, Yingtong Dou, Philip S. Yu, Yutong Deng, and Hao Peng. 2020. Alleviating the Inconsistency Problem of Applying Graph Neural Network to Fraud Detection. In *Proceedings of the 43rd International ACM SIGIR conference on research and development in Information Retrieval, SIGIR 2020, Virtual Event, China, July 25-30, 2020*, Jimmy Huang, Yi Chang, Xueqi Cheng, Jaap Kamps, Vanessa Murdock, Ji-Rong Wen, and Yiqun Liu (Eds.). ACM, 1569–1572. https://doi.org/10.1145/3397271.3401253
[60] Moshe Looks, Marcello Herreshoff, DeLesley Hutchins, and Peter Norvig. 2017. Deep Learning with Dynamic Computation Graphs. In *ICLR*. OpenReview.net.
[61] Elio Lozano and Edgar Acuña. 2005. Parallel Algorithms for Distance-Based and Density-Based Outliers. In *ICDM*. IEEE Computer Society, 729–732.
[62] Emaad Manzoor, Hemank Lamba, and Leman Akoglu. 2018. xstream: Outlier detection in feature-evolving data streams. In *KDD*. ACM, 1963–1972.
[63] Chen Meng, Minmin Sun, Jun Yang, Minghui Qiu, and Yang Gu. 2017. Training deeper models by GPU memory optimization on TensorFlow. In *Proc. of ML Systems Workshop in NIPS*. NIPS.
[64] Prashanth Menon, Todd C Mowry, and Andrew Pavlo. 2017. Relaxed operator fusion for in-memory databases: Making compilation, vectorization, and prefetching work together at last. *VLDB* 11, 1 (2017), 1–13.
[65] Seung Won Min, Vikram Sharma Mailthody, Zaid Qureshi, Jinjun Xiong, Eiman Ebrahimi, and Wen-mei Hwu. 2020. EMOGI: efficient memory-access for out-of-memory graph-traversal in GPUs. *VLDB* 14, 2 (2020), 114–127.
[66] Seung Won Min, Kun Wu, Sitao Huang, Mert Hidayetoğlu, Jinjun Xiong, Eiman Ebrahimi, Deming Chen, and Wen Mei Hwu. 2021. Large graph convolutional network training with GPU-oriented data communication architecture. *VLDB* 14, 11 (2021), 2087–2100.
[67] Supun Nakandala, Karla Saur, Gyeong-In Yu, Konstantinos Karanasos, Carlo Curino, Markus Weimer, and Matteo Interlandi. 2020. A Tensor Compiler for Unified Machine Learning Prediction Serving. In *OSDI*. OSDI, 899–917.
[68] Deepak Narayanan, Aaron Harlap, Amar Phanishayee, Vivek Seshadri, Nikhil R. Devanur, Gregory R. Ganger, Phillip B. Gibbons, and Matei Zaharia. 2019. PipeDream: Generalized Pipeline Parallelism for DNN Training. In *Proceedings of the 27th ACM Symposium on Operating Systems Principles* (Huntsville, Ontario, Canada) *(SOSP '19)*. Association for Computing Machinery, New York, NY, USA, 1–15. https://doi.org/10.1145/3341301.3359646
[69] Henry Neeb and Christopher Kurrus. 2016. Distributed k-nearest neighbors.
[70] Graham Neubig, Yoav Goldberg, and Chris Dyer. 2017. On-the-fly Operation Batching in Dynamic Computation Graphs. In *NeurIPS*. 3971–3981.
[71] Junki Oku, Keiichi Tamura, and Hajime Kitakami. 2014. Parallel processing for distance-based outlier detection on a multi-core CPU. In *IEEE International Workshop on Computational Intelligence and Applications (IWCIA)*. IEEE, 65–70.
[72] Gustavo H Orair, Carlos HC Teixeira, Wagner Meira Jr, Ye Wang, and Srinivasan Parthasarathy. 2010. Distance-based outlier detection: consolidation and renewed bearing. *VLDB* 3, 1-2 (2010), 1469–1480.
[73] Matthew Eric Otey, Amol Ghoting, and Srinivasan Parthasarathy. 2006. Fast Distributed Outlier Detection in Mixed-Attribute Data Sets. *Data Min. Knowl. Discov.* 12, 2-3 (2006), 203–228. https://doi.org/10.1007/s10618-005-0014-6
[74] Guansong Pang, Chunhua Shen, Longbing Cao, and Anton Van Den Hengel. 2021. Deep learning for anomaly detection: A review. *CSUR* 54, 2 (2021), 1–38.
[75] Spiros Papadimitriou, Hiroyuki Kitagawa, Phillip B. Gibbons, and Christos Faloutsos. 2003. LOCI: Fast Outlier Detection Using the Local Correlation Integral. In *ICDE*. IEEE Computer Society, 315–326.
[76] Adam Paszke, Sam Gross, Francisco Massa, Adam Lerer, James Bradbury, Gregory Chanan, Trevor Killeen, Zeming Lin, Natalia Gimelshein, Luca Antiga, et al. 2019. Pytorch: An imperative style, high-performance deep learning library. *NeuIPS* 32 (2019), 8026–8037.
[77] Fabian Pedregosa, Gaël Varoquaux, Alexandre Gramfort, Vincent Michel, Bertrand Thirion, Olivier Grisel, Mathieu Blondel, Peter Prettenhofer, Ron Weiss, Vincent Dubourg, et al. 2011. Scikit-learn: Machine learning in Python. *the Journal of machine Learning research* 12 (2011), 2825–2830.
[78] Tomás Pevný. 2016. Loda: Lightweight on-line detector of anomalies. *Mach. Learn.* 102, 2 (2016), 275–304.
[79] Sebastian Raschka. 2015. *Python machine learning*. Packt publishing ltd.
[80] Hansheng Ren, Bixiong Xu, Yujing Wang, Chao Yi, Congrui Huang, Xiaoyu Kou, Tony Xing, Mao Yang, Jie Tong, and Qi Zhang. 2019. Time-series anomaly detection service at microsoft. In *Proceedings of the 25th ACM SIGKDD international conference on knowledge discovery & data mining*. ACM, 3009–3017.
[81] Petar Ristoski, Christian Bizer, and Heiko Paulheim. 2015. Mining the Web of Linked Data with RapidMiner. *J. Web Semant.* 35 (2015), 142–151. https://doi.org/10.1016/j.websem.2015.06.004
[82] Lukas Ruff, Robert A. Vandermeulen, Nico Görnitz, Alexander Binder, Emmanuel Müller, Klaus-Robert Müller, and Marius Kloft. 2020. Deep Semi-Supervised Anomaly Detection. In *8th International Conference on Learning Representations, ICLR 2020, Addis Ababa, Ethiopia, April 26-30, 2020*. OpenReview.net. https://openreview.net/forum?id=HkgH0TEYwH
[83] Bernhard Schölkopf, John C. Platt, John Shawe-Taylor, Alexander J. Smola, and Robert C. Williamson. 2001. Estimating the Support of a High-Dimensional Distribution. *Neural Comput.* 13, 7 (2001), 1443–1471.
[84] Erich Schubert, Arthur Zimek, and Hans-Peter Kriegel. 2014. Generalized Outlier Detection with Flexible Kernel Density Estimates. In *SDM*. SIAM, 542–550.
[85] Mei-Ling Shyu, Shu-Ching Chen, Kanoksri Sarinnapakorn, and LiWu Chang. 2003. *A novel anomaly detection scheme based on principal component classifier*. Technical Report.
[86] Petru Sincraian. 2021. PyOD Download Statistics. https://pepy.tech/project/pyod. Accessed: 2021-09-09.
[87] Martin Svedin, Steven Wei Der Chien, Gibson Chikafa, Niclas Jansson, and Artur Podobas. 2021. Benchmarking the Nvidia GPU Lineage: From Early K80 to Modern A100 with Asynchronous Memory Transfers. In *HEART '21*. ACM, 9:1–9:6.
[88] Nguyen Thanh Tam, Matthias Weidlich, Bolong Zheng, Hongzhi Yin, Nguyen Quoc Viet Hung, and Bela Stantic. 2019. From anomaly detection to rumour detection using data streams of social platforms. *VLDB* 12, 9 (2019), 1016–1029.
[89] Jian Tang, Zhixiang Chen, Ada Wai-Chee Fu, and David Wai-Lok Cheung. 2002. Enhancing Effectiveness of Outlier Detections for Low Density Patterns. In *PAKDD (Lecture Notes in Computer Science)*, Vol. 2336. Springer, 535–548.
[90] Theodoros Toliopoulos, Christos Bellas, Anastasios Gounaris, and Apostolos Papadopoulos. 2020. PROUD: PaRallel OUtlier Detection for Streams. In *Proceedings of the 2020 International Conference on Management of Data, SIGMOD Conference 2020, online conference [Portland, OR, USA], June 14-19, 2020*, David Maier, Rachel Pottinger, AnHai Doan, Wang-Chiew Tan, Abdussalam Alawini, and Hung Q. Ngo (Eds.). ACM, 2717–2720. https://doi.org/10.1145/3318464.3384688
[91] Luan Tran, Min Y Mun, and Cyrus Shahabi. 2020. Real-time distance-based outlier detection in data streams. *VLDB* 14, 2 (2020), 141–153.
[92] Colin Unger, Zhihao Jia, Wei Wu, Sina Lin, Mandeep Baines, Carlos Efrain Quintero Narvaez, Vinay Ramakrishnaiah, Nirmal Prajapati, Pat McCormick, Jamaludin Mohd-Yusof, Xi Luo, Dheevatsa Mudigere, Jongsoo Park, Misha Smelyanskiy, and Alex Aiken. 2022. Unity: Accelerating DNN Training Through Joint Optimization of Algebraic Transformations and Parallelization. In *16th USENIX Symposium on Operating Systems Design and Implementation (OSDI 22)*. USENIX Association, Carlsbad, CA, 267–284. https://www.usenix.org/conference/osdi22/presentation/unger
[93] Haojie Wang, Jidong Zhai, Mingyu Gao, Zixuan Ma, Shizhi Tang, Liyan Zheng, Yuanzhi Li, Kaiyuan Rong, Yuanyong Chen, and Zhihao Jia. 2021. PET: Optimizing Tensor Programs with Partially Equivalent Transformations and Automated Corrections. In *OSDI*. OSDI, 37–54.
[94] Mengzhao Wang, Xiaoliang Xu, Qiang Yue, and Yuxiang Wang. 2021. A Comprehensive Survey and Experimental Comparison of Graph-Based Approximate Nearest Neighbor Search. *Proc. VLDB Endow.* 14, 11 (2021), 1964–1978. https://doi.org/10.14778/3476249.3476255

[95] Runhui Wang and Dong Deng. 2020. DeltaPQ: lossless product quantization code compression for high dimensional similarity search. *VLDB* 13, 13 (2020), 3603–3616.

[96] Shuang Wang and Hakan Ferhatosmanoglu. 2020. PPQ-trajectory: spatio-temporal quantization for querying in large trajectory repositories. *VLDB* 14, 2 (2020), 215–227.

[97] Yizhou Yan, Lei Cao, Caitlin Kulhman, and Elke Rundensteiner. 2017. Distributed local outlier detection in big data. In *KDD*. ACM, 1225–1234.

[98] Susik Yoon, Jae-Gil Lee, and Byung Suk Lee. 2019. NETS: extremely fast outlier detection from a data stream via set-based processing. *VLDB* 12, 11 (2019), 1303–1315.

[99] Rose Yu, Huida Qiu, Zhen Wen, ChingYung Lin, and Yan Liu. 2016. A survey on social media anomaly detection. *SIGKDD Explorations* 18 (2016), 1–14.

[100] Aoqian Zhang, Shaoxu Song, Jianmin Wang, and Philip S Yu. 2017. Time series data cleaning: From anomaly detection to anomaly repairing. *VLDB* 10, 10 (2017), 1046–1057.

[101] Sean Zhang, Varun Ursekar, and Leman Akoglu. 2022. Sparx: Distributed Outlier Detection at Scale. *arXiv preprint arXiv:2206.01281* (2022).

[102] Yue Zhao. 2021. PyOD Citation Statistics. https://scholar.google.ca/scholar?cites=3726241381117726876&as_sdt=5,39&sciodt=0,39&hl=en. Accessed: 2021-09-09.

[103] Yue Zhao, Xiyang Hu, Cheng Cheng, Cong Wang, Changlin Wan, Wen Wang, Jianing Yang, Haoping Bai, Zheng Li, Cao Xiao, Yunlong Wang, Zhi Qiao, Jimeng Sun, and Leman Akoglu. 2021. SUOD: Accelerating Large-Scale Unsupervised Heterogeneous Outlier Detection. In *Proceedings of Machine Learning and Systems 2021, MLSys 2021, virtual, April 5-9, 2021*, Alex Smola, Alex Dimakis, and Ion Stoica (Eds.). mlsys.org. https://proceedings.mlsys.org/paper/2021/hash/98dce83da57b0395e163467c9dae521b-Abstract.html

[104] Yue Zhao, Zain Nasrullah, Maciej K. Hryniewicki, and Zheng Li. 2019. LSCP: Locally Selective Combination in Parallel Outlier Ensembles. In *Proceedings of the 2019 SIAM International Conference on Data Mining, SDM 2019, Calgary, Alberta, Canada, May 2-4, 2019*, Tanya Y. Berger-Wolf and Nitesh V. Chawla (Eds.). SIAM, 585–593. https://doi.org/10.1137/1.9781611975673.66

[105] Yue Zhao, Zain Nasrullah, and Zheng Li. 2019. PyOD: A Python Toolbox for Scalable Outlier Detection. *JMLR* 20 (2019), 96:1–96:7.

[106] Qiwei Zhong, Yang Liu, Xiang Ao, Binbin Hu, Jinghua Feng, Jiayu Tang, and Qing He. 2020. Financial defaulter detection on online credit payment via multi-view attributed heterogeneous information network. In *WWW*. ACM, 785–795.

SUPPLEMENTARY MATERIAL FOR TOD

Details on system design and experiments.

A DEMO ON USING TOD TO IMPLEMENT NEW OD ALGORITHMS FROM SCRATCH

Overview of implementing new OD algorithms with TOD . As shown in §4, TOD takes a modular approach to implement an OD algorithm. Thus, using TOD to implement a new OD algorithm requires conceptualizing the algorithm as a combination of operators (BTOs and FOs) in TOD (see Fig. 2). Thanks to the nature of OD applications that do not involve complex optimization, most OD algorithms can be decomposed as a combination of 2 to 3 operators.

Overview of ECOD . We provide an example of using TOD to implement the latest OD algorithm with empirical cumulative distribution functions (ECOD) [53], which is just published in early 2022. In a nutshell, ECOD estimates the empirical distribution of each feature (i.e., density estimation), where it considers that outliers locate in low-density regions. After that, ECOD aggregates all density estimation results per feature into final outlier scores.

Turning ECOD into abstraction. ECOD mainly involves two operators: (*i*) it estimates the density ("`f. Density est.`") of each features by "`8. Basic OPs (ECDF)`" and (*ii*) then aggregates density results across all features via "`7. Agg.`". By having the process in mind, we could sketch the abstraction of ECOD in Fig. A1.

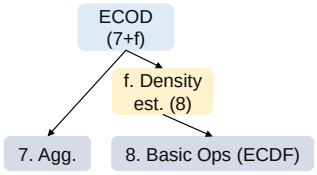

Figure A1: Examples of building latest OD algorithm ECOD with FOs and BTOs conveniently.

Turning abstraction into code . We provide the code breakdown to show how to use TOD to implement ECOD, and the full implementation is available for further reference. The code snippet (i) shows that we use the basic operator ECDF for density estimation and (ii) shows the aggregation step of density estimation as outlier scores. Putting these core parts together with some skeleton code, we could conveniently include ECOD in TOD. It is noted that we still need to glue the operators together, while the use of predefined TOD operators helps us to achieve acceleration.

```
from .basic_operators import ecdf_multiple

# density estimation via ECDF
self.U_l = ecdf_multiple(X, device=self.device)
self.U_r = ecdf_multiple(-X, device=self.device)
```

(i) code of density estimation in ECOD

```
# take the negative log
self.U_l = -1 * torch.log(self.U_l)
self.U_r = -1 * torch.log(self.U_r)

# aggregate and generate outlier scores
self.O = torch.maximum(self.U_l, self.U_r)
self.decision_scores_ = torch.sum(self.O,
    dim=1).cpu().numpy() * -1
```

(ii) code of density aggregation in ECOD

B EXAMPLE OF USING TOD TO BUILD CLASSIFICATION ALGORITHMS

As discussed in §8, TOD may be used to construct algorithms beyond OD, e.g., classification and regression. In this section, we demonstrate the use of TOD to build a popular classifier called k nearest neighbor classifiers (kNN_CLF)[26].

In short, kNN_CLF is a lazy classifier and does not involve a training stage. For a test sample $\mathbf{X}_{\text{test}}$, it calculates the pairwise distance between the test sample with each "training" data. It then uses the aggregation (e.g., majority vote or avg.) to decide the predicted classes of each test sample. Thus, it can be decomposed as the combination of (i) calculating pairwise distance by `cdist` (ii) identifying the top k neighbors by `topk` and (iii) predicting the class labels by aggregating the labels from the neighbors (i.e., `Basic OPs`).

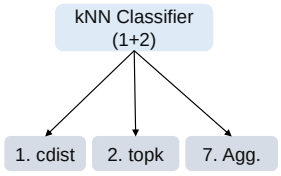

Figure B2: Examples of building kNN classifier with TOD

Table B1 provides a detailed comparison between CPU-based implementation of kNN_CLF in scikit-learn (sklearn) [77] and TOD's implementation. On average, TOD's kNN_CLF is 10.1 times faster than that of sklearn due to the GPU acceleration.

Table B1: Runtime (in seconds) comparison of kNN classifier using CPU-based scikit-learn (sklearn) [77] vs. GPU-enabled TOD. On average, TOD's implementation is 10.1 times faster than that of sklearn.

Train Size	Test Size	Number of Features	kNN-sklearn	kNN-TOD
50,000	50,000	100	41.35	4.76
50,000	50,000	200	52.26	4.83
100,000	50,000	100	84.84	8.09
100,000	50,000	200	88.13	8.36

C ADDITIONAL EXPERIMENT RESULTS

C.1 End-to-end Results on Synthetic Datasets

Consistent with the results presented in §7.3, TOD **is significantly faster than the leading CPU-based system on large synthetic datasets**. Fig. C3 shows the results on three synthetic datasets (where Synthetic 1 contains 100,000 samples, Synthetic 2 contains 200,000 samples, and Synthetic 3 contains 400,000 samples (all are with 200 features). The results show that TOD is on average 10.9× faster than PyOD on the five benchmark algorithms (13.0×, 15.9×, 9.3×, 7.2×, and 8.9× speed-up on LOF, kNN, ABOD, HBOS, and PCA, respectively).

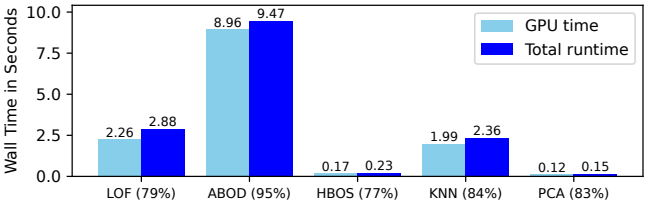

(a) Synthetic dataset 1 (20,000 samples with 200 features)

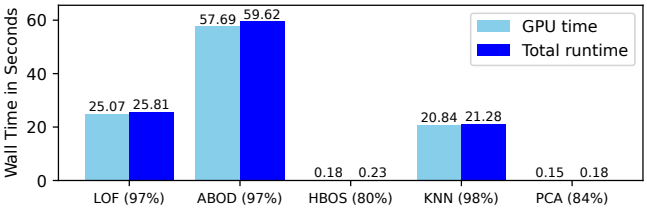

(b) Synthetic dataset 2 (100,000 samples with 200 features)

Figure C4: GPU time and total runtime of TOD **in seconds on synthetic datasets (where the percentage is shown in parenthesis).** TOD **achieves significant efficiency improvement with high GPU usages (e.g., mostly** > 80%**)**

.

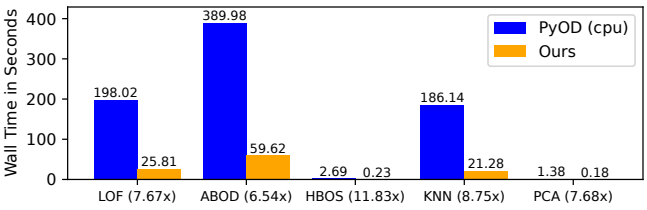

(a) Synthetic dataset 1 (100,000 samples with 200 features)

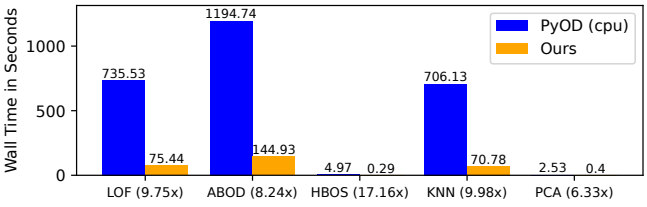

(b) Synthetic dataset 2 (200,000 samples with 200 features)

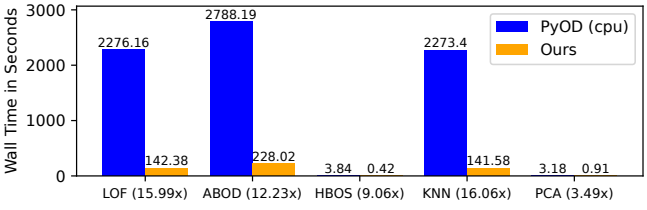

(c) Synthetic dataset 3 (400,000 samples with 200 features)

Figure C3: Runtime comparison between PyOD and TOD **in seconds on synthetic datasets (see §7.3 Fig. 8 for results on real-world datasets).** TOD **significantly outperforms PyOD in all w/ much smaller runtime, where the speedup factor is shown in parenthesis by each algorithm. On avg.,** TOD **is 10.9× faster than PyOD (up to 38.9×)**

.

C.2 Further Time Analysis

Fig. C4 shows the comparison between GPU time and the total runtime, where GPU time consists of a large portion of the total runtime, and verifies that the acceleration of TOD mainly comes from the use of GPU(s). Moreover, we also notice that the GPU efficiency increases for larger datasets with higher percentages. This also explains why we observe more acceleration of TOD on large datasets in Fig. 8 and Appx. Fig. C3.

C.3 Case Study on Operator Fusion

Although automatic batching applies to all BTOs and FOs, we introduce an additional technique called operator fusion in §6.1 to further optimize the execution of selected operators in sequence. For instance, *k*NN batching is achieved by running `cdist` and `topk` sequentially, where each uses automatic batching and the output of the former is the input of the latter.

Differently, we could further optimize this simple concatenation execution by fusing `cdist` and `topk` together for better efficiency. Fig. 7 compares simple concatenation (subfigure a) and operator fusion (subfigure b) on *k*NN. Specifically, the latter executes the `topk` BTO on the `cdist` BTO's individual batches separately rather than running `topk` on the full distance matrix outputted by `cdist`. This prevents moving the entire $n \times n$ distance matrix between operators, which often causes OOM.

In Table C2, we compare the performance of simple concatenation (i.e., `cdist` and then `topk`) and operator fusion regarding both GPU memory and time consumption, where operator fusion shows great performance improvement.

Table C2: GPU memory consumption (in Mb) and runtime (in seconds) comparison of simple concatenation (SC) and operator fusion (OF) for *k*NN. Operator fusion brings huge savings in both GPU memory consumption and runtime.

Sample Size	GPU-SC	GPU-OF	Runtime-SC	Runtime-OF
50,000	5280	3060	8.47	2.80
100,000	9010	3060	33.48	9.12

C.4 Ablation Studies on Provable Quantization and Automatic Batching

In addition to the end-to-end analysis in §7.3, we also provide further ablations on provable quantization (PQ) and automatic batching (AB) in this section. We demonstrate this experiment with *k*–NN OD algorithm where both techniques apply. Table C3 shows that automatic batching addresses the issue of out-of-memory on large datasets, while provable quantization reduces GPU memory consumption and runtime. The ablations show that using both techniques leads to the best performance.

Table C3: Ablations on provable quantization (PQ) and automatic batching (AB) for kNN. We set batch size equal to 40,000, and thus AB does not apply to the first row of the table. The best performing combination is highlighted in bold, where using both techniques achieves the best performance.

# Samples	PQ&AB	AB only	PQ only	None
40,000	**5.34**	N/A	5.34	10.88
80,000	**15.12**	20.91	17.56	OOM
160,000	**45.37**	67.22	OOM	OOM

(a) Runtime in seconds

# Samples	PQ&AB	AB only	PQ only	None
40,000	**3,040**	N/A	**3040**	12,170
80,000	**3,040**	12,050	12,020	OOM
160,000	**3,040**	12,050	OOM	OOM

(b) GPU memory consumption in Mb

D OPEN-SOURCE SYSTEM AND API DEMONSTRATION

Accessibility. To facilitate accessibility of TOD, we release it under the open BSD 2 license[1], which can be easily installed via Python Package Index (PyPI)[2] with name `pytod`.

API design and demonstration. Follow by the mature API design of scikit-learn [20] and PyOD [105], all the supported OD algorithms have a unified API design: (*i*) `fit` processes the input data and calculates necessary statistics for prediction, where the outlier scores are also calculated on the input data (*ii*) `decision_function` returns the raw outlier scores of newcoming samples based on the fitted outlier detector in the inductive setting and (*iii*) `predict` returns the binary labels of newcoming samples based on the fitted outlier detector. We demonstrate these APIs in TOD with kNN detector below, and other supported OD algorithms have the same APIs.

[1]Github Repo: https://github.com/yzhao062/pytod

[2]Python Package Index (PyPI: https://pypi.org/project/pytod/

```
from pytod.utils.data import generate_data
from pytod.utils.data import evaluate_print
from pytod.models.knn import KNN

# Generate sample data
X_train, y_train, X_test, y_test = \
    generate_data(n_train=50000, n_test=10000)

device = validate_device(0) # get the GPU 0

# initialize a kNN model in TOD with k=10 and
     batch=10000
clf = KNN(n_neighbors=k, batch_size=10000,
     device=device)

# fit the kNN model
clf.fit(X_train)

# get the train labels and outlier scores
y_train_scores = clf.decision_scores_ # raw outlier
     scores
y_train_pred = clf.labels_ # binary labels

# evaluate and print the results
evaluate_print(clf_name, y_train, y_train_scores)

# get the prediction labels and outlier scores on test
y_test_scores = clf.decision_function(X_test) # raw
     scores
```

API demo of invoking kNN in TOD; other OD algorithms follow the same API design

Utility functions. To facilitate system comparison and evaluation, we also create a set of helper functions including (*i*) `generate_data` that can creates synthetic OD datasets by modeling normal samples by Gaussian distribution and outliers by uniform distribution and (*ii*) `evaluate_print` to provide OD specific evaluations by the metrics described in §7.2.